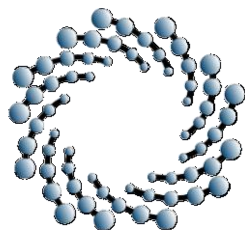

INSTITUTO POTOSINO DE INVESTIGACIÓN CIENTÍFICA Y TECNOLÓGICA, A.C.

POSGRADO EN CIENCIAS EN BIOLOGIA MOLECULAR

Análisis de la regulación del proteoma de *Ustilago maydis* por dimorfismo, pH y los genes *MAPK* y *GCN5*

Tesis que presenta

José Luis Martínez Salgado

Para obtener el grado de

Doctor en Ciencias en Biología Molecular

Codirectores de la Tesis:

Dra. Ana Paulina Barba de la Rosa

Dr. José Ruiz Herrera

San Luis Potosí, S.L.P., Febrero 2013

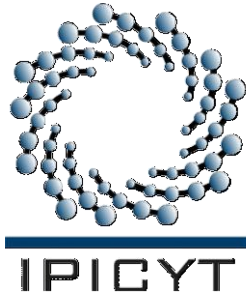

Constancia de aprobación de la tesis

La tesis **"Análisis de la regulación del proteoma de *Ustilago maydis* por dimorfismo, pH y los genes MAPK y GCN5"** presentada para obtener el Grado de de Doctor en Ciencias en Biología Molecular fue elaborada por **José Luis Martínez Salgado** y aprobada el **21 de febrero de 2013** por los suscritos, designados por el Colegio de Profesores de la División de Biología Molecular del Instituto Potosino de Investigación Científica y Tecnológica, A.C.

____
Dra. Ana Paulina Barba de la Rosa
(Codirector de tesis)

____
Dr. José Ruiz Herrera
(Codirector de tesis)

____
Dr. Alejandro de las Peñas Nava
(Miembro del Comité Tutoral)

____
Dr. Sergio Casas Flores
(Miembro del Comité Tutoral)

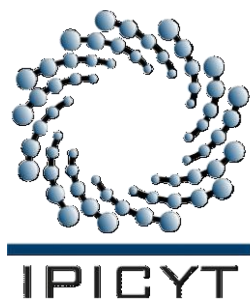

Créditos Institucionales

Esta tesis fue elaborada en el Laboratorio de Proteómica y Biomedicina Molecular de la División de Biología Molecular del Instituto Potosino de Investigación Científica y Tecnológica, A.C., bajo la codirección de la Dra. Ana Paulina Barba de la Rosa y el Dr. José Ruiz Herrera).

Durante la realización del trabajo el autor recibió una beca académica del Consejo Nacional de Ciencia y Tecnología 175592.

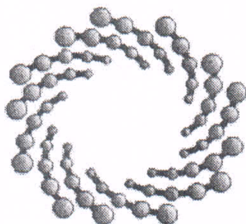

IPICYT

Instituto Potosino de Investigación Científica y Tecnológica, A.C.

Acta de Examen de Grado

El Secretario Académico del Instituto Potosino de Investigación Científica y Tecnológica, A.C., certifica que en el Acta 051 del Libro Primero de Actas de Exámenes de Grado del Programa de Doctorado en Ciencias en Biología Molecular está asentado lo siguiente:

En la ciudad de San Luis Potosí a los 21 días del mes de febrero del año 2013, se reunió a las 12:00 horas en las instalaciones del Instituto Potosino de Investigación Científica y Tecnológica, A.C., el Jurado integrado por:

Dr. José Ruiz y Herrera	**Presidente**	**CINVESTAV Irapuato**
Dr. J. Sergio Casas Flores	**Secretario**	**IPICYT**
Dr. Alejandro De Las Peñas Nava	**Sinodal**	**IPICYT**
Dra. Ana Paulina Barba de la Rosa	**Sinodal**	**IPICYT**

a fin de efectuar el examen, que para obtener el Grado de:

DOCTOR EN CIENCIAS EN BIOLOGÍA MOLECULAR

sustentó el C.

José Luis Martínez Salgado

sobre la Tesis intitulada:

Análisis de la regulación del proteoma de Ustilago maydis por dimorfismo, pH y los genes MAPK y GCN5

que se desarrolló bajo la dirección de

Dra. Ana Paulina Barba de la Rosa
Dr. José Ruiz y Herrera (CINVESTAV Irapuato)

El Jurado, después de deliberar, determinó

APROBARLO

Dándose por terminado el acto a las 13:30 horas, procediendo a la firma del Acta los integrantes del Jurado. Dando fe el Secretario Académico del Instituto.

A petición del interesado y para los fines que al mismo convengan, se extiende el presente documento en la ciudad de San Luis Potosí, S.L.P., México, a los 21 días del mes de febrero de 2013.

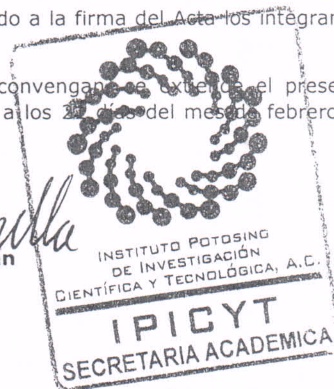

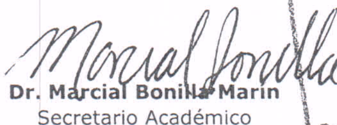

Dr. Marcial Bonilla Marín
Secretario Académico

Mtra. Ivonne Lizette Cuevas Vélez
Jefa del Departamento del Posgrado

Agradecimientos

Al consejo Nacional de Ciencia y Tecnología por la beca otorgada

A la Dra. Ana Paulina Barba de la Rosa y al Dr. José Ruiz Herrera por su dirección y asesoría en este trabajo

A mi comité tutorial los doctores Alejandro de las Peñas Nava y Sergio Casas Flores

Al apoyo técnico de Alberto Barrera y de Claudia León

A mis compañeros Laboratorio de Proteómica y Biomedicina Molecular

Contenido

Constancia de aprobación de la tesis ii
Créditos institucionales iii
Acta de examen iv
Agradecimientos v
Lista de tablas viii
Lista de figuras ix
Resumen x
Abstract xi

I. Introducción 1
- 1.1. Ustilaginales 1
- 1.2. Dimorfismo 3
- 1.3. *Ustilago maydis* 7
- 1.4. Señales que afectan la morfología y virulencia 9
- 1.5. Proteómica 14

II. Justificación 19
III. Objetivos 20
- 3.1. Objetivo general 20
- 3.2. Objetivos específicos 20

IV. Metodologia 21
- 4.1. Cultivo de cepas e inducción del dimorfismo 21
- 4.2. Extracción de proteínas 21
- 4.3. Electroforesis bidimensional 22
- 4.4. Análisis de imágenes 22
- 4.5. Digestión en gel 22
- 4.6. Espectrometría de masas 23
- 4.7. Búsqueda en base de datos 23

V. Resultados 25

5.1. Analysis of the regulation of the *Ustilago maydis* proteome by dimorphism, pH or *MAPK* and *GCN5* genes 25
VI. Conclusiones 71
VII. Referencias 72

Lista de tablas

Tabla 1. Algunos factores ambientales o genéticos que causan la transición entre el crecimiento en forma de micelio y levadura 4

Tabla 2. Estudios en hongos para aplicaciones biotecnológicas o en la agricultura 18

Lista de figuras

Figura 1. Algunos Ustilaginales que causan carbones en cultivos importantes. 1
Figura 2. Formas celulares de *Ustilago.* 2
Figura 3. Patogénesis del dimorfismo de basidiomicetos. 5
Figura 4. Dimorfismo en *U. maydis* inducido por cambio de pH. 6
Figura 5. El *Ustilago maydis* como alimento. 7
Figura 6. Interacción entre los dos loci de tipo de apareamiento durante el desarrollo de *U. maydis*. 10
Figura 7. Vias de señalización cAMP y MAPK durante el apareamiento y la invasión de la planta. 11
Figura 8. Efecto del pH en la via de cAMP. 12
Figura 9. Identificación de genes específicos involucrados en el dimorfismo. 13
Figura 10. Esquema de la electroforesis de doble dimensión. 15
Figura 11. Estrategia general en el análisis proteómico. 16

Resumen

Análisis de la regulación del proteoma de *Ustilago maydis* por dimorfismo, pH y los genes *MAPK* y *GCN5*

Ustilago maydis es un hongo basidiomycota patógeno del maíz. Sus células haploides son capaces de crecer en forma de levadura en un medio de cultivo líquido con un pH de 7, mientras que a un pH de 3 presenta un crecimiento en forma de micelio. Se utilizaron geles de electroforesis bidimensional acoplados a LC ESI/MS-MS para el análisis de proteínas diferencialmente acumuladas en las formas de levadura y micelio. Los mapas 2-DE fueron obtenidos en el rango de 5-8 donde un total de 404 spots proteicos fueron separados, de estos, 43 fueron diferencialmente acumulados cuando se compararon las cepas (FB2*wt* y las mutantes monomórficas CL211 para levadura y GP25 para micelio) creciendo a pH de 7 contra pH 3. Las topoisomerasa 2, tioredoxin peroxidasa y Vdac fueron sobre acumuladas en la forma de micelio mientras que la proteína de unión a ADN Hpm1 y la aldo ceto reductasa disminuyeron su acumulación. En CL211 varios factores de transcripción como Btf3a disminuyen su acumulación lo cual podría estar relacionado con la via de MAPK, mientras que la mutacion en *gcn5* (GP25) muestra la disminución en la acumulación de Mge1 y Lpd1-dihidrolipoamida deshidrogenasa. Lys12 fue sobre acumulada en la forma de micelio de FB2*wt* y GP25, esta proteína ha sido reportada como un nuevo blanco para antifungicos. Se identifico la sobreacumulación de CipC y la disminución en la acumulación de Hmp1 como proteínas especificas relacionadas con el dimorfismo cuando las proteínas afectadas por el cambio en el pH fueron descartadas. Nuestros resultados complementan la información de los genes y proteínas relacionados con la transición dimórfica en *U. maydis*.

PALABRAS CLAVE: mutantes constitutivas; dimorfismo; proteomica; pH; geles de electroforesis bidimensional; *Ustilago maydis*

Abstract

Analysis of the regulation of the *Ustilago* 1 *maydis* proteome by dimorphism, pH or *MAPK* and *GCN5* genes

Ustilago maydis is a dimorphic corn pathogenic basidiomycota. *U. maydis* haploid cells are able to grow in liquid synthetic where at pH 7 grows as yeast, while at pH 3 it develops in the mycelial form. Two-dimensional gel electrophoresis coupled with LC ESI/MS-MS was used to analyze the differential accumulation of proteins in the yeast and the mycelial morphologies. 2-DE maps were obtained in the pH range of 5-8 where 404 total protein spots were separated, from these 43 were differentially accumulated when comparing strains (FB2*wt* and constitutive yeast or mycelial mutants, CL211 and GP25, respectively) growing at pH 7 against pH 3. Topoisomerase2, thioredoxin, and Vdac were up-accumulated in mycelial form while Hpm1 DNA binding protein and aldo keto reductase were down-accumulated. The down-accumulation in CL211 of several transcription factors such as Btf3a, could be related with the MAPK pathway, while mutation in *gcn5* (GP25) was reflected in the down-accumulation of Mge1 and Lpd1-dihydrolipoamide dehydrogenase. Lys12 was up-accumulated in the mycelial form in both FB2*wt* and GP25 at pH 3. This protein has been reported as a new target for antifungal drugs. Specific proteins related to dimorphism were found when proteins affected by changes in the medium pH were eliminated; then dimorphism was related with the up-accumulation of CipC and down-accumulation of Hmp1.Our results complement the information about the genes and proteins related with the dimorphic transition in *U. maydis*.

KEY WORDS: constitutive mutants; dimorphism; proteomics; pH; two-dimensional gel electrophoresis; *Ustilago maydis*

I. INTRODUCCION

1.1 Ustilaginales

El orden de los Ustilaginales pertenece al Phylum Basidiomycota y a la clase de los Teliomycetes y comprende aproximadamente 1200 especies distribuidas en más de 50 géneros, son un grupo vasto y diverso de hongos en los que se incluyen los carbones, denominados de este modo por la formación de masas negras de esporas, semejantes al carbón, que presentan al fructificar. Son patógenos de las plantas y causan perdidas en los cultivos en todo el mundo, e infectan aproximadamente 4000 especies de angiospermas distribuidas en 75 familias de plantas (Martínez-Espinoza y col. 2002). Muchos carbones tienen un estrecho rango de huésped y están especializados en miembros de las Poaceae (gramíneas) las cuales incluyen especies de cultivos importantes como el maíz, sorgo, azúcar de caña, trigo y cebada (Fig. 1) (Brefort y col., 2009).

Figura 1. Algunos Ustilaginales que causan carbones en cultivos importantes

Los ustilaginales pueden desarrollarse en tallos, hojas, flores, frutos y semillas de las plantas huéspedes. En los tejidos vegetales el micelio comúnmente se desarrolla de forma intercelular. Carecen de basidiocarpo (pero ver adelante), pueden formar soros o agallas grandes, en donde se producen las teliosporas. Las teliosporas se forman de células intercalares del micelio dicarionte, el cual con frecuencia, presenta fíbulas, según las especies (Fig. 2). En su mayor parte son heterotálicos bipolares o tetrapolares. No presentan órganos sexuales de manera que la plasmogamia se efectúa mediante la fusión de células compatibles, ya sean basidiosporas, conidios, células hifales o esporas con células hifales (Herrera y Ulloa, 1998).

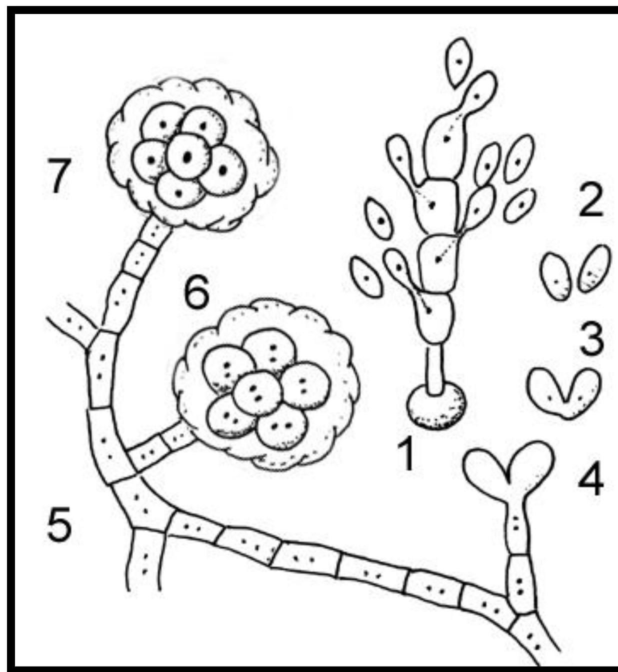

Figura 2. Formas celulares de *Ustilago*: 1. Telíospora germinando, 2. Basidiosporas, 3. Somatogamia entre basidiósporas, 4. Desarrollo de micelio dicariótico, 5. Micelio dicariótico desarrollado, 6. Vesículas con teliosporas binucleadas, 7. Telíosporas uninucleadas. (www.hongosyplantas.es)

1.2 Dimorfismo

El dimorfismo fúngico es un fenómeno reversible por el cual un hongo puede pasar de una forma de micelio a forma de levadura o viceversa en función de las condiciones ambientales (Sánchez y Pérez, 2001). Numerosos hongos patógenos de humanos y plantas exhiben este fenómeno, de tal manera que la patogenicidad es usualmente limitada por una morfología particular. El control entre estos patrones de crecimiento requiere de una organización coordinada del citoesqueleto y el tráfico de vesículas para restablecer la polaridad celular y dirigir la síntesis de pared celular (Mahlert y col*.,* 2006).

El fenómeno del dimorfismo no está limitado para algún grupo taxonómico, este es compartido por especies representativas de los Phyla Basiodiomycota, Ascomycota y Zygomycota (Morales-Vargas y col., 2012). El cambio entre micelio y levadura en hongos dimórficos como respuesta a factores ambientales puede inducirse experimentalmente como se muestra en la Tabla 1. Diversos patógenos oportunistas del hombre se desarrollan en forma de micelio como los saprofitos de las plantas y en el laboratorio mantienen esta morfología en cultivos con temperaturas de 20-25 °C. Pero estos se convierten en levaduras en los fluidos del cuerpo o cuando en el laboratorio se incuban a 37 °C. Este dimorfismo regulado térmicamente es un factor significativo en la patogénesis (Deacon, 2006).

Tabla 1. Algunos factores ambientales o genéticos que causan la transición entre el crecimiento en forma de micelio y levadura.

Hongo	Condiciones para forma de micelio	Condiciones para forma de levadura
Patógenos del hombre		
Histoplasma capsulatum	20-25 °C	37 °C
Blastomyces dermatitidis	20-25 °C	37 °C
Paracoccidioides brasiliensis	20-25 °C	37 °C
Sporothrix schenckii	20-25 °C	37 °C
Coccidioides immitis	20-25 °C	37 °C
Candida albicans	Bajos niveles de nutrientes	Altos niveles de nutrientes
Saprofitos		
Mucor rouxii y algunos otros Zygomicotas	Aireación	Anaerobiosis
Patógenos de plantas		
Ophiostoma ulmi	Calcio Algunas fuentes de nitogeno.	Baja concentración de calcio
Ustilago maydis	Dicarionte	Monocarionte
Patógenos de insectos		
Metarhizium anisopliae	Medio sólido	Cultivo liquido
Beauveria bassiana	Medio sólido	Cultivo liquido

(Adaptada de Deacon. 2006).

Muchas levaduras sexuales en los basidiomycota tienen un ciclo de vida dimórfico (Fig. 3). Inicialmente, una basidiospora haploide germina para producir la levadura de vida libre. En este estado puede colonizar una gran variedad de sustratos en suelos o hábitats acuáticos. En la presencia de otra célula compatible se produce la formación de tubos de conjugación que finalmente fusionan las células para producir una hifa dicarionte. Los basidiomicota mantienen un estado prolongado de dicarionte, donde cada célula posee dos núcleos parentales sin fusionar. La fusión y meiosis ocurre en un basidio para producir una tétrada de basidioesporas haploides (Morrow y Fraser 2009).

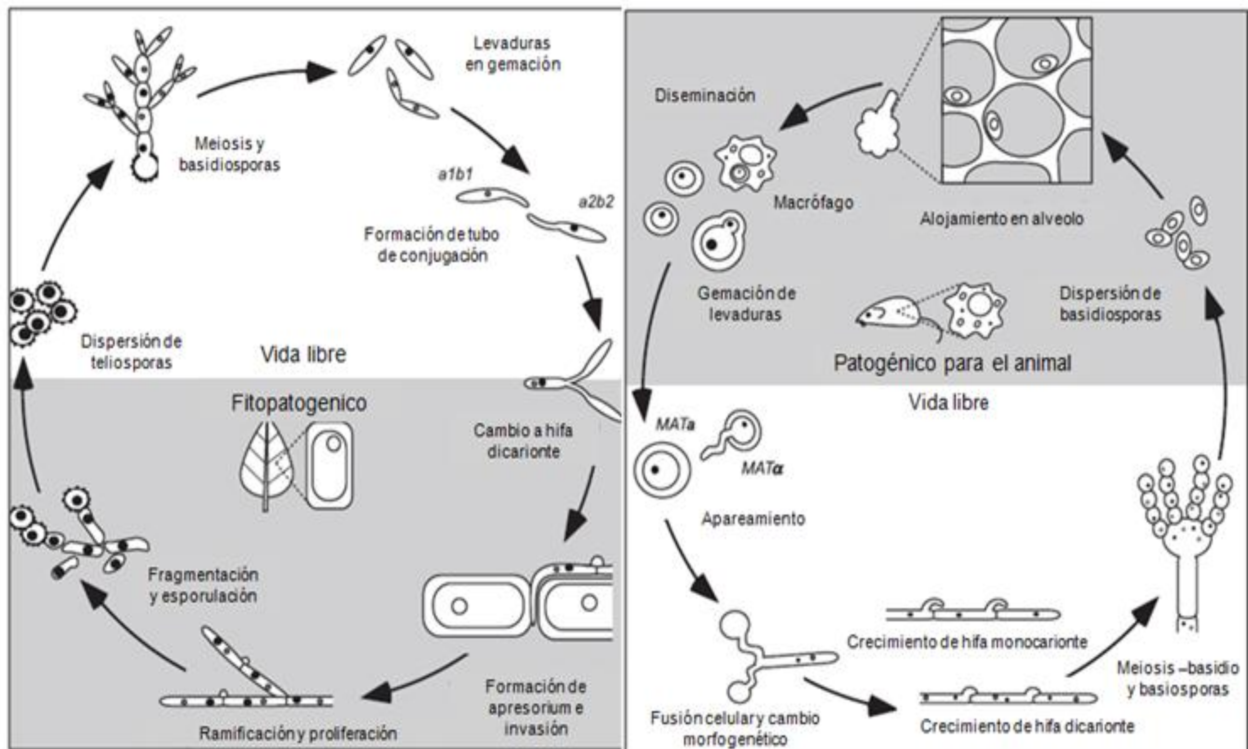

Figura 3. Patogénesis del dimorfismo de basidiomicetos. La forma de levadura de *Ustilago maydis* (izquierda) es no patógena, hasta el apareamiento con otra compatible para realizar el cambio morfológico al forma infecciosa de hifa e invadir la planta. La célula de *Cryptococcus neoformans* (derecha) cambia a una hifa dicarionte la cual puede encontrase en vida libre. La cariogamia ocurre en el basidio, donde las basidiosporas son producidas. La reproducción sexual y el respectivo cambio dimórfico son cruciales para iniciar la infección de una planta o animal (Adaptado de Morrow y Fraser, 2008).

El pH extracelular es uno de los factores ambientales que afecta la diferenciación morfológica del patógeno oportunista *Candida albicans*. La habilidad para responder a medios neutro-alcalino es controlada por las vías de traducción de señales, que activan el factor de la transcripción Rim 101. La ruta RIM101/PacC, que dirige las respuestas a pH y de diferenciación, también ha sido estudiada en *Saccharomyces cerevisiae* y *Aspergillus nidulans* (Davis, 2003).

La transición dimórfica de *U. maydis in vitro* ocurre en cepas haploides o diploides como respuesta al pH externo (Fig. 4). A un pH neutro el hongo crece como una población homogénea de levaduras, mientras que a pH ácido este desarrolla una forma micelial. (Aréchiga y Ruiz, 2004). La obtención de mutantes con una deleción del gen *RIM101* mostró que la ruta Pal/Rim es funcional en *U. maydis*, donde como en otros hongos, controla una serie de funciones celulares pero no está involucrada en el dimorfismo inducido por pH (Aréchiga-Carvajal y Ruiz-Herrera, 2005).

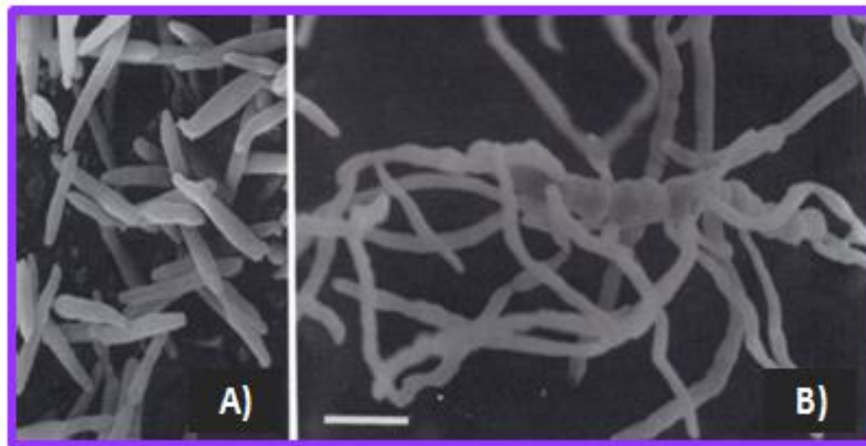

Figura 4. Dimorfismo en *U. maydis* inducido por cambio de pH. A) Levaduras a pH 7. B) Micelio a pH 3 (tomado de Ruiz-Herrera y col., 1995).

1.3 *Ustilago maydis*

En México es muy abundante el cultivo de maíz y, frecuentemente se observa parasitado por el hongo *Ustilago maydis* comúnmente llamado huitlacoche (huitlacoche) del náhuatl cui= excremento, tlaloe=maíz, “excremento del maíz”; (Bonifaz, 2000).

El carbón que invade la mazorca del maíz conocido como “huitlacoche” ha sido preparado como un platillo comestible desde el periodo precolombino en la parte central de México y es ya importante en la industria alimenticia. Además de ser considerado un platillo de lujo en restaurantes con un notable éxito a nivel internacional (Fig. 5) (Ruiz-Herrera y Martínez-Espinoza, 1998).

Figura 5. El *Ustilago maydis* como alimento. Conocido como “huitlacoche” es empleado en la preparación de una gran variedad de platillos en México.

U. maydis es un hongo basidiomycota patógeno del maíz (*Zea mays*) y su progenitor el teozintle (*Zea mays* subsp. *parviglumis*). Su ciclo de vida normal que ocurre en la naturaleza implica una etapa sexual. Las células haploides se multiplican vegetativamente por gemación y son saprofitas; capaces de infectar plantas. La fusión de células haploides sexualmente compatibles es necesaria para la formación de un dicarionte, el cual crece en forma de hifa y es estrictamente dependiente de la planta huésped para sustentar su desarrollo. El micelio prolifera formando grandes tumores o agallas, y el desarrollo patogénico se complementa con la producción de grandes cantidades de teliosporas diploides ricas en melanina. Estas esporas se distribuyen por el aire y pueden germinar bajo condiciones favorables, Después de pasar por meiosis, se producen esporidios haploides unicelulares (Bölker, 2001). En condiciones controladas en la que cepas diploides o mezclas de haploides sexualmente compatibles se incuban junto a callos embriogénicos de maíz, se desarrolla un ciclo de vida totalmente diferente, en la que se forman basidiocarpos (en contra de lo que generalmente se acepta). En los basidiocarpos ocurre la meiosis con formación de holobasidias, contrariamente a lo que ocurre en el ciclo de vida natural donde se forman fragmobasidias (Cabrera-Ponce y col., 2012).

Durante los últimos 15 años *U. maydis* ha sido un modelo muy importante para el estudio molecular de los mecanismos de fitopatogenicidad causada por hongos. Las investigaciones moleculares se han enfocado en la recombinación, el papel del apareamiento (*mating*) en la patogénesis y las vías de señalización que influencian la virulencia. De igual manera se ha utilizado en el estudio de un número importante de procesos celulares tales como la señalización, regulación transcripcional y post-transcripcional, regulación del ciclo celular así como la recombinación y reparación del DNA (Vollmeister y col., 2011).

Los análisis bioinformaticos demuestran que *U. maydis* se encuentra más relacionado a los humanos que otros organismos fúngicos modelo. Un numero alto de proteínas se comparten solo entre *U. maydis* y *H. sapiens*. Existe evidencia que sugiere que los principios de transporte a larga distancia, mitosis y la organización

de microtúbulos están conservados entre *U. maydis* y humanos, por lo cual es un sistema atractivo para el estudio de ciertos procesos en mamíferos (Steinberg y Perez, 2007).

El tamaño del genoma de *U. maydis* es de aproximadamente 20.5 Mb y contiene 6902 genes que codifican proteínas. Una observación importante es que posee pocos genes involucrados en la degradación de tejido vegetal vivo o muerto como polisacárido hidrolasas, polisacárido liasas y pectin esterarsas. *U. maydis* posee solo 33 enzimas hidrolíticas en contraste con las 138 y 103 presentes en *Magnaporthe grisea* y *Fusarium graminearum*, respectivamente. Esto concuerda perfectamente con el estilo biotrófico de *U. maydis*, en el cual el daño al huésped debe ser mínimo (Kämper y col., 2006). El genoma se encuentra disponible en la base de datos de MIPS (http://mips.helmholtz-muenchen.de/genre/proj/ustilago/).

1.4 Señales que afectan la morfología y la virulencia

En *U. maydis* las células haploides de tipo de apareamiento compatible se reconocen por medio de feromonas lipopépticas específicas y se fusionan para formar el dicarionte infeccioso. Este proceso está regulado por el *locus* de tipo de apareamiento "*a*" (Fig. 6). Esta unión induce un cambio morfogenético de levadura a un crecimiento filamentoso. La formación de filamento y la del desarrollo patogénico son coordinadamente controlados por el *locus* multialélico de tipo de apareamiento "*b*", el cual codifica un homeodominio de factores de trascripción que actúan como heterodímeros (Kämper y col.,1995). La formación del complejo es genéticamente controlada y restringida a las proteínas bE y bW codificadas por diferentes alelos del *locus b*. De esta manera se garantiza que la actividad del heterodímero se forme solamente en el dicarionte y no se genere en células haploides. (Feldbrügge y col., 2004).

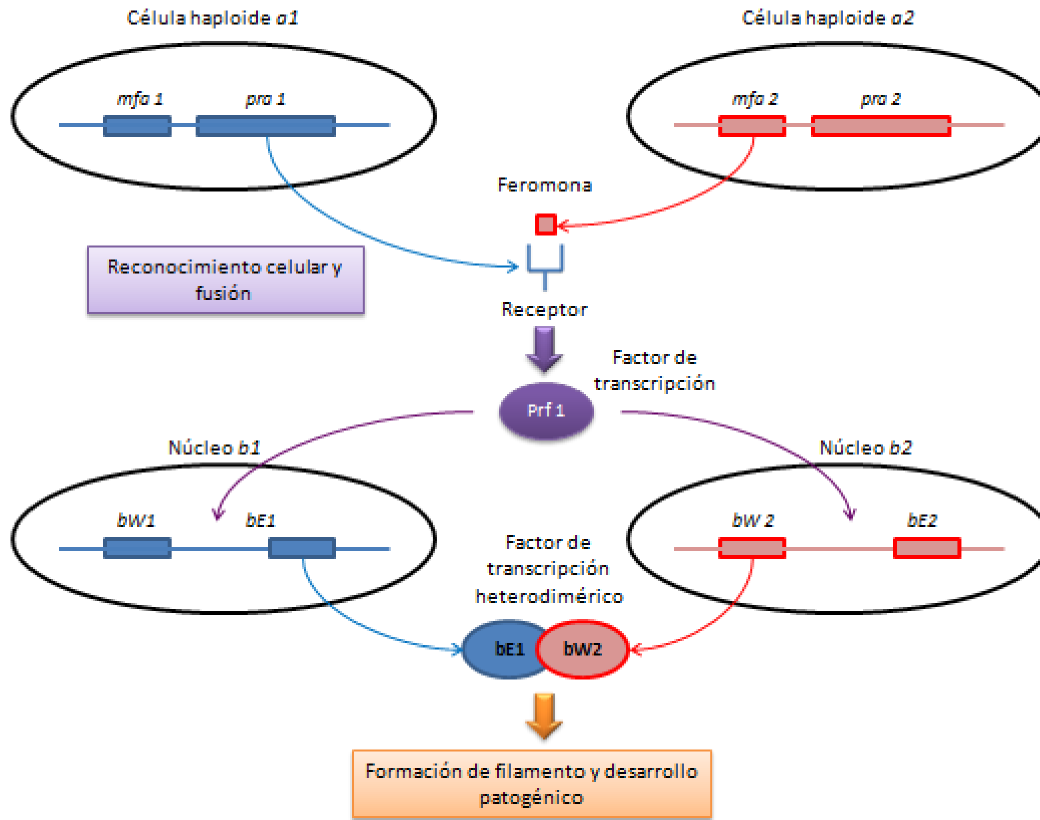

Figura 6. Interacción entre los dos *loci* de tipo de apareamiento durante el desarrollo de *U. maydis*. El *locus* bialelico *a* codifica un sistema de reconocimiento feromona-receptor, el cual dispara la fusión de las células, Posteriormente los diferentes alelos en el multi alelico *locus b*, inducen el desarrollo patogénico por la formación de un factor de transcripción heterodimérico (adaptada de Bölker, 2001).

Durante el apareamiento, cuando las feromonas son detectadas comienzan a actuar dos cascadas de señalización muy conservadas: la ruta de la proteína cinasa A (PKA) dependiente de AMP cíclico y una vía de MAPK cinasa (proteína cinasa activada por mitógeno, por sus siglas en inglés). Los componentes de estas vías cruciales se muestran en la Figura 7. Después de la activación inducida por feromonas, ambas vías convergen en el factor de transcripción clave Prf1, el cual induce la transcripción de un grupo grande de genes que incluye a los genes de tipo de apareamiento de los *locus a* y *b* (Zarnack y col., 2008). Para inducir la expresión de los genes *MFA* y *PRA*, Prf1 necesita estar fosforilado por Adr1 mediante la vía PKA, mientras que la inducción de los genes del *locus b* requiere que Prf1 esté fosforilado por Adr1 y Kpp2 de la vía MAPK (Kaffarnik y col., 2003).

Además, la transcripción de *PRF1* está regulada por dos miembros de la vía MAPK, Kpp2 y Crk1 mediante una interacción compleja de al menos cuatro factores de transcripción río abajo que se unen a elementos discretos del promotor del gen *PRF1*: Prf1 (auto regulación), Rop1, Hap2 y un factor aun sin identificar rio abajo de Crk1 (Brefort y col., 2009).

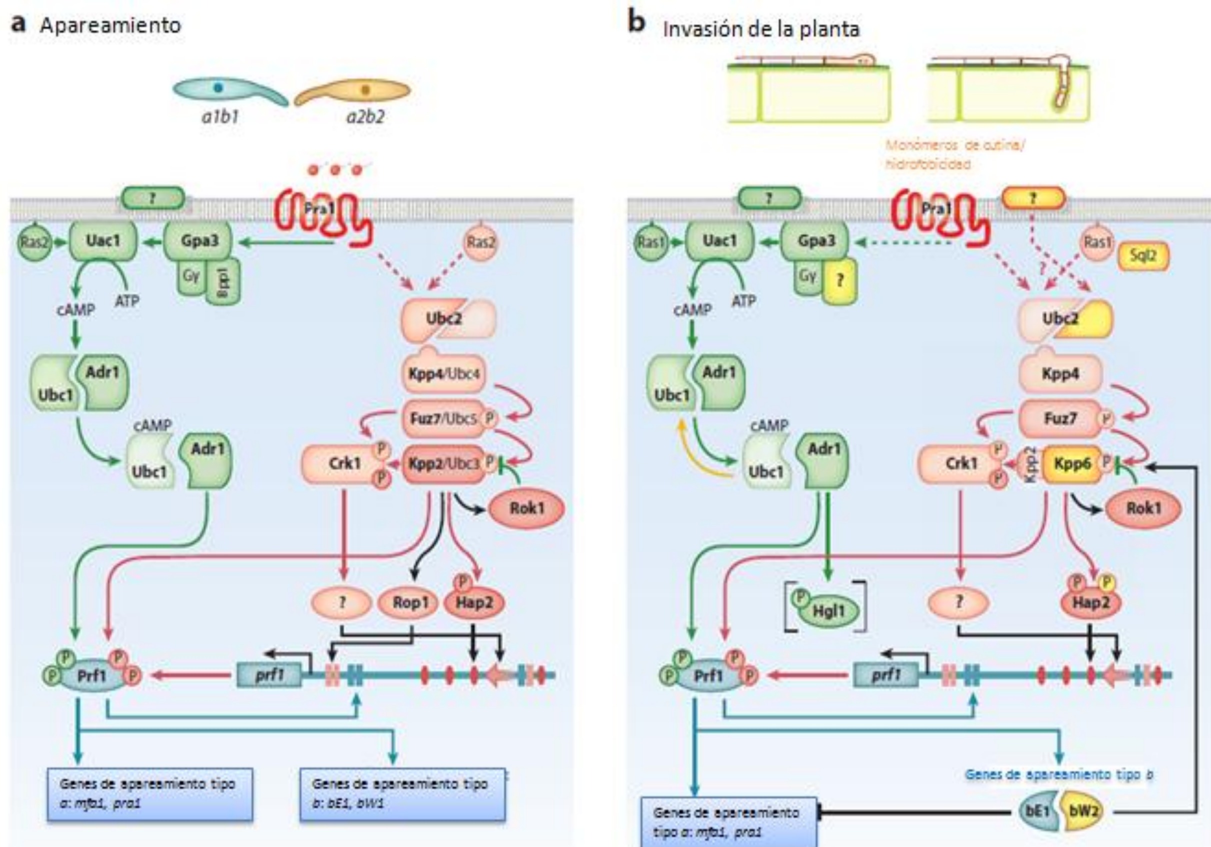

Figura 7. Vias de señalización cAMP y MAPK durante el apareamiento y la invasión de la planta. Los componentes de cAMP (verde) y de MAPK (rojo) son señalados y sus interacciones son señaladas con flechas de color semejante. Los círculos con la letra P indican fosoforilación. (a) Componentes requeridos para el apareamiento en una célula haploide *a1b1*. (b) Componentes requeridos para el desarrollo patogénico del dicarionte. Los componentes que son requeridos específicamente durante la patogénesis son remarcados en amarillo (Adaptado de Brefort y col., 2009).

Excepto por la fosfatasa recientemente identificada Rok1, todos los componentes mostrados en la Figura 7a son necesarios para una fusión eficiente de células en un cultivo axénico. El análisis de mutantes en cepas que contienen los alelos compatibles del *locus b* ha revelado que muchos de los componentes requeridos por la señalización de feromonas, juegan un papel adicional durante la patogénesis. Esto indica que los principales componentes de las vías cAMP y MAPK transmiten señales de la planta, además de las feromonas. Aunque, algunos componentes adicionales se requieren exclusivamente para la patogénesis, otros no son indispensables (Fig. 7*a* y 7*b*) (Brefort y col., 2009).

Se ha visto que que la inducción por pH del crecimiento en forma de micelio en *U. maydis* está influenciada por las vías MAPK y cAMP (Martínez-Espinoza y col. 2004). Se plantea que la adenilato ciclasa (Uac1) es inhibida por un pH ácido y se reduce la síntesis *de novo* de cAMP (Fig. 8). La hoja del maíz provee de condiciones acidas que contribuyen a la inducción de la filamentación. Se sugiere que *U. maydis* indirectamente puede precipitar la reducción localizada del pH sobre el apoplasto de la planta al producir auxinas y de esta forma retroalimenta la inducción del crecimiento filamentoso.

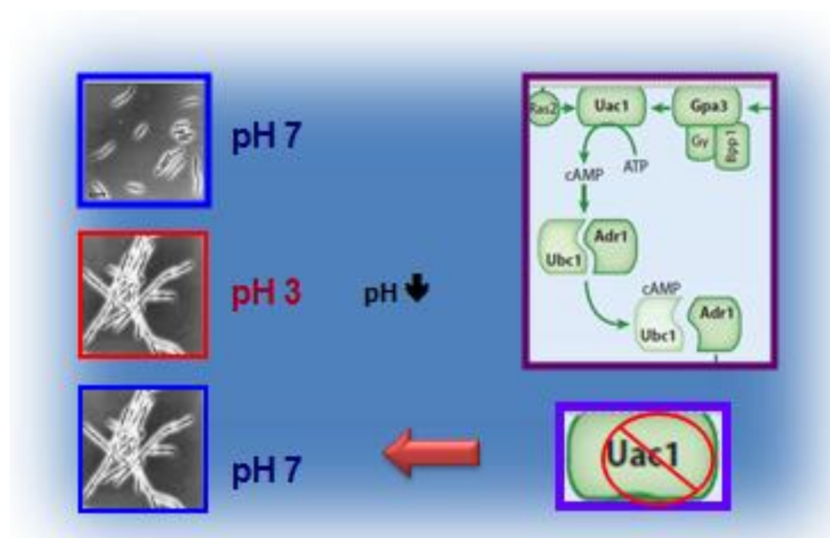

Figura 8. Efecto del pH en la vía de cAMP. La adenilatociclasa (Uac1) inhibida por un pH ácido o eliminada de una cepa haploide induce la filamentación de *U. maydis* (adaptado de Martínez-Espinoza y col., 2004).

Para poder realizar un análisis de genes o proteínas involucradas en transición de levadura a micelio al disminuir el pH del medio es importante el considerar que dicho cambio afectará a otros genes o proteínas específicos distintos a los de la formación de micelio por el pH ácido. Robledo-Briones y Ruiz-Herrera (2012) realizaron la búsqueda de genes involucrados en la síntesis y estructura de la pared celular de *U. maydis* durante su transición dimórfica por el cambio en el pH. Gracias al uso de dos mutantes las cuales mantienen su morfología independientemente del pH (monomórficas): GP25, mutante micelio constitutiva, deficiente en un gen que codifica para la acetilasa de histonas Gcn5 (Gonzalez-Prieto y col., en preparación) y CL211, mutante levadura constitutiva, deficiente en un gen que codifica para la Map cinasa Ubc2 (Martínez-Espinoza y col., 1997). Los genes diferencialmente expresados se agruparon mediante diagramas de Venn (Fig. 9). Cada elemento de este diagrama tiene en común la comparación entre la morfología de levadura y micelio. De esta forma se identifican los genes que fueron específicamente regulados durante el dimorfismo independientemente del pH del medio.

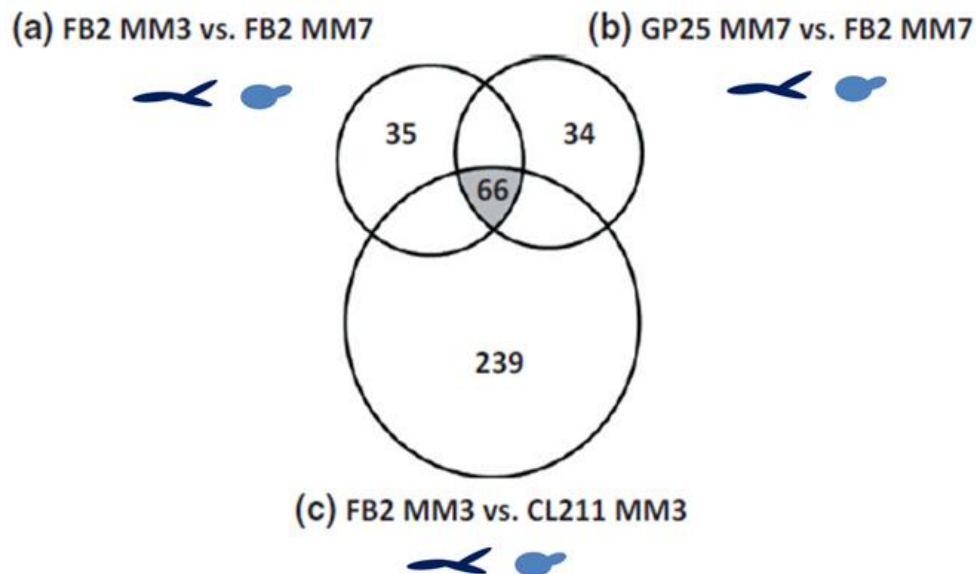

Figura 9. Identificación de genes específicos involucrados en el dimorfismo. El diagrama de Venn muestra el número de genes encontrados con expresión diferencial en las comparaciones indicadas. (a) FB2*wt* a pH 3 vs pH 7; (b) FB2 a pH7 vs GP25 a pH 7; (c) FB2 a pH 3 vs CL211 a pH 3. La zona gris muestra el número de genes que están específicamente relacionados en el dimorfismo (Adaptado de Robledo-Briones y Ruiz-Herrera, 2012).

De igual manera, el uso de mutantes monomórficas como controles y el empleo de diagramas de Venn para separar diversos efectores fue empleado en la identificación de los genes involucrados en la transición dimórfica de levadura a micelio por cambio en el pH en *Yarrowia lipolytica* (Morales-Vargas y col., 2012).

1.5 Proteómica

Para entender los procesos biológicos a nivel molecular, es necesario visualizar la actividad y la interacción de las proteínas. Para su estudio se han desarrollado técnicas que permiten su separación, cuantificación y determinación de sus características individuales. Una de las técnicas más importantes de separación empleadas en la actualidad es la electroforesis, la cual involucra el movimiento de proteínas cargadas a través de una matriz bajo la influencia de un campo eléctrico aplicado. En la década de los 50's el desarrollo en el campo de la electroforesis tuvo un gran auge especialmente con el uso de geles de acrilamida, Esta técnica se continua utilizando para la separación de proteínas, en particular los geles de electroforesis de poliacrilamida con dodecilsulfato de sodio (SDS-PAGE, por sus siglas en inglés) (Westermeier y col., 2002).

La proteómica es la caracterización a gran escala de las proteínas completas de una línea celular, tejido u organismo (Graves y Haystead, 2002). Los estudio proteómicos consisten principalmente de dos tipos de técnicas: técnicas de separación y caracterización de proteínas mediante la espectrometría de masas (Aebersold y Mann, 2003). Estas técnicas se unen a la bioinformática para el análisis, interpretación e integración de la enorme cantidad de datos obtenidos.

La electroforesis de doble dimensión es un método muy utilizado en el análisis de mezclas compleja de proteínas extraídas de diversas muestras biológicas. Esta técnica separa las proteínas en base a dos propiedades independientes en dos pasos consecutivos: la primera dimensión consiste en un isoelectroenfoque por el cual las proteínas se separan en base a su punto isoeléctrico (p*I*); la segunda dimensión es la separación de las proteínas conforme

a su peso molecular relativo (Mr) mediante una electroforesis en un gel de poliacrilamida con SDS. Cada punto en el gel 2D resultante corresponde a una especie de proteína en la muestra. Miles de diferentes proteínas pueden ser separadas y la información específica para cada proteína puede ser obtenida (Fig. 10).

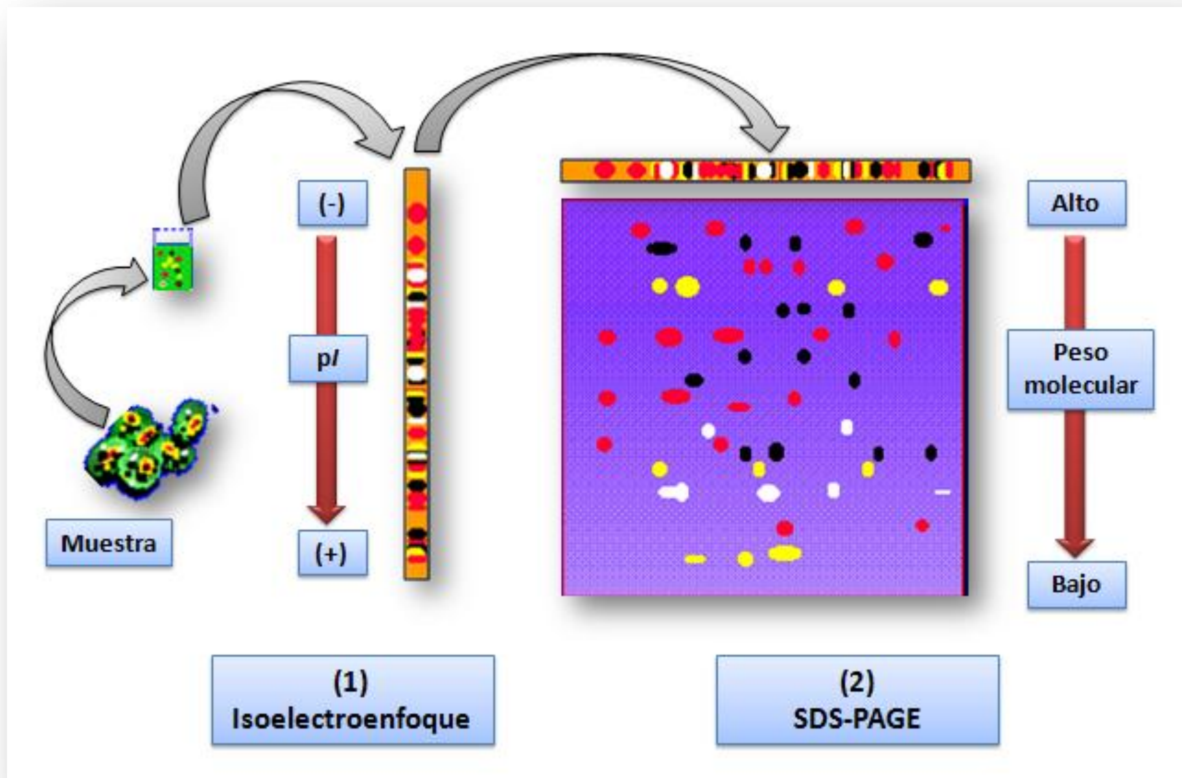

Figura 10. Esquema de la electroforesis de doble dimensión. La mezcla de proteínas obtenida es separada (1) de acuerdo al punto isoeléctrico de cada proteína en una tira de isoelectroenfoque. Posteriormente una segunda separación de acuerdo al peso molecular se realiza en un gel de poliacrilamida (2).

El análisis proteómico comprende tres pasos principales (Fig. 11), cada uno empleando diferentes tecnologías. El paso inicial y más importante es el manejo de las muestras para la electroforesis en dos dimensiones (2D). El segundo paso es la digitalización de las imágenes y el análisis de los patrones electroforéticos. La tercera etapa es la identificación y caracterización de las proteínas por espectrometría de masas (Lee, 2001).

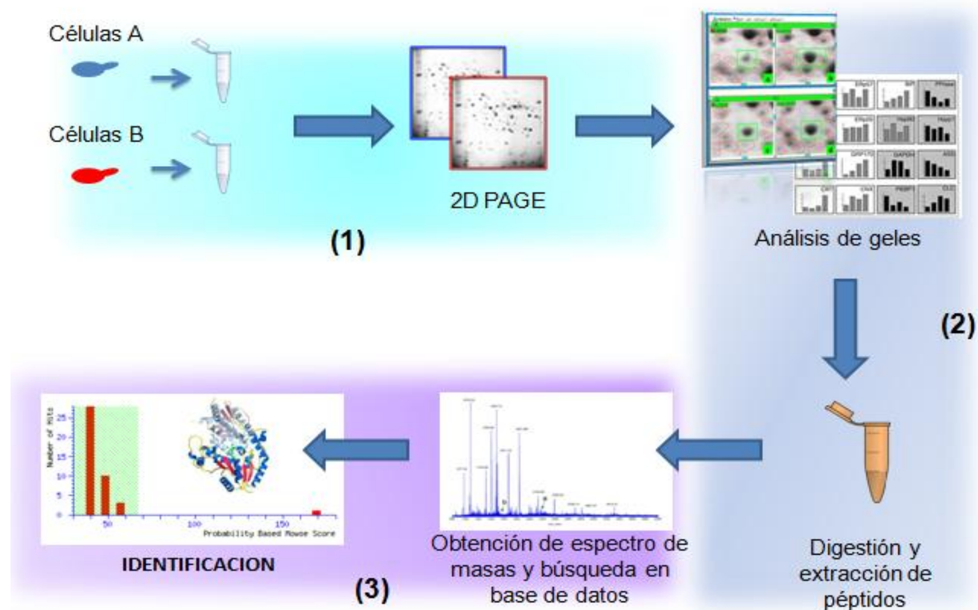

Figura 11. Estrategia general en el análisis proteómico: (1) Separación de las proteínas en geles 2D. (2) Análisis de los patrones electroforéticos. (3) Identificación de proteínas por espectrometría de masas

La espectrometría de masas se ha convertido en el método más utilizado para la identificación de proteínas a gran escala. Es una técnica analítica que permite conocer la masa molecular de un analito, como un péptido, de una forma muy precisa. Se basa en la formación de iones de un analito en fase gaseosa, que serán separados y detectados según su relación masa/carga (m/z), lo que dará lugar en última instancia a un espectro de masas en el que se representa la abundancia relativa de cada uno de estos iones en función de su m/z. Tras la digestión de una proteína (comúnmente con tripsina) se obtiene un conjunto de péptidos de tamaños determinados por su secuencia de aminoácidos. Los espectros generados por las masas de los péptidos son comparados con las masas teóricas de las digestiones de las proteínas de las bases de datos. Cuantos más péptidos experimentales coincidan con los teóricos, mayor probabilidad existe de que la proteína identificada sea la correcta (Cabezón, 2009)

Mediante la electroforesis de doble dimensión y el análisis por espectrometría de masas, se ha contribuido en gran manera a la investigación experimental de los proteomas de sistemas biológicos complejos. Estas herramientas tienen éxito al estudiar la cantidad y localización subcelular de proteínas individuales, para examinar los cambios en los patrones de expresión entre las diferentes fases de crecimiento y en la respuesta a estímulos, o a identificar genes blanco de proteínas reguladoras (Vitali y col., 2005).

Con la finalidad de entender la interacción entre plantas y patógenos, se han realizado estudios (Tabla 2) donde la proteómica es parte de un análisis integrativo multidisciplinario, que se extiende desde el estudio de los genes hasta la observación de un genotipo, pasando por proteínas y metabolismo. Por otro lado los estudios de patogenicidad de los hongos generan información que ha permitido la identificación de factores de virulencia, la caracterización de rutas de señalización y vías bioquímicas. De esta forma se descubren nuevos blancos para el diagnóstico de enfermedades en cultivos o el diseño de fungicidas (González y col., 2010).

El enfoque proteómico ha servido para el estudio de la transición dimórfica como una de las estrategias de virulencia del patógeno oportunista *C. albicans*. Esto ha permitido realizar análisis de las interacciones funcionales de las proteínas diferencialmente abundantes, para mostrar los procesos metabólicos y de reorganización celular durante la transición de levadura a hifa y así proponer un modelo de reorganización metabólica (Monteoliva y col., 2011).

Respecto al dimorfismo de *U. maydis* Böhmer y col. (2007) realizaron un análisis proteómico de la transición dimórfica de *U. maydis* mediante la sobreexpresión del heterodimero bW2/bE1 así como la sobreexpresión de Rac1, una proteína de unión a GTP. Estos autores describieron 13 proteínas que presentan un incremento en la intensidad de la mancha proteica después de inducir el crecimiento filamentoso. De estas manchas, solo cuatro fueron compartidas por los dos sistemas inducibles.

Tabla 2. Estudios en hongos para aplicaciones biotecnológicas o en la agricultura.

Hongo	Trabajos
Boletus edilus	Estrés salino de este hongo micorriza por su importancia en la reforestación en aéreas salinas.
Coprinopsis cinérea ***Pleorotus ostreatus*** ***Phanerochaete chrysosporium*** ***Polyporus brumalis*** ***Schizophyllum commune***	Optimización de un protocolo 2D para proteínas extracelulares de hongos degradadores de madera.
Glomus intraradices	Simbiosis micorriza arbuscular.
Metarhizium anisopliae	Actividad bioinsecticida para la producción de plantas resistentes a plagas de insectos.
Monascus pilosus	Influencia de las limitaciones de nitrógeno en la producción industrial de policetidos.
Phanerochaete chrysosporium	Procesos ligninolíticos para la industria de la pulpa de celulosa.
Trichoderma atroviride ***T. harzianum*** ***T. reesei***	Propiedades como agentes de biocontrol.
Amanita bisporigera	Estudio de las enzimas que degradan la pared celular.

(Adaptada de González y col., 2009).

II. JUSTIFICACION

El crecimiento continuo de la población mundial demanda una enorme cantidad de alimentos y el aumento en el uso de cultivos vegetales para la obtención de biocombustibles, convierten a las enfermedades fúngicas que afectan las plantas, como uno de los retos más importantes para la agricultura. Esto genera la necesidad de desarrollar cultivos con resistencia a este estrés biótico. Para lograr esto, los mecanismos que utilizan los hongos patógenos para colonizar las plantas necesitan ser elucidados. (Djamei y Kahmann, 2012).

El modelo de interacción planta-patógeno de *Ustilago maydis* ofrece la ventaja de que los pasos iniciales de la infección en la planta, el dimorfismo, pueden ser simulados *in vitro*. Aunado a esto, el acceso a la secuencia de su genoma facilita la identificación de proteínas cuya abundancia cambia en este proceso mediante técnicas proteómicas.

III. OBJETIVOS

3.1 Objetivo General

Analizar los cambios en la expresión de proteínas en *Ustilago maydis* por la transición dimórfica inducida por cambio de pH, bajo el control del pH y afectadas por la mutación en la vía MAPK, o en una acetilasa de histonas. Se usaran las cepas haploides silvestre, FB2wt, GP25 micelio constitutiva y CL211 levadura constitutiva.

3.2 Objetivos Específicos

- Estandarizar la extracción de proteínas de la cepa silvestre *FB2wt* en su forma de levadura y micelio inducido por pH, así como de las cepas CL211 y GP25 bajo las mismas condiciones.
- Obtener el intervalo de pH ideal para una mejor distribución en la separación por punto isoeléctrico.
- Identificar las diferencias en los patrones bidimensionales de expresión de las proteínas.
- Encontrar las proteínas cuya regulación está afectada por el cambio en el pH, el dimorfismo o bajo el control de las vías indicadas, mediante la sustracción y representación del análisis en diagramas de Venn
- Caracterizar por espectrometría de masas la identidad de las proteínas diferenciales.
- Elucidar los posibles mecanismos biológicos que son afectados por la transición dimórfica inducida, así como aquellos que se ven afectados por el cambio en el pH y las mutaciones de las cepas monomórficas.

IV. METODOLOGIA

4.1 Cultivo de cepas e inducción del dimorfismo

Las cepas utilizadas fueron: FB2*wt U. maydis* (Banuett & Herskowitz, 1989) y como control las mutantes monomórficas: GP25, mutante micelio constitutiva, deficiente en un gen que codifica para la acetilasa de histonas Gcn5 (Gonzalez-Prieto y col., en preparación) y CL211, mutante levadura constitutiva, deficiente en un gen que codifica para la Map cinasa Ubc2 (Martínez-Espinoza y col., 1997). Las cepas se mantuvieron a -70ºC en 50% (v/v) glicerol. Las células fueron recuperadas en medio completo Holliday (1974). Posteriormente la transición fue realizada en medio mínimo Holliday con un pH de 7 o de 3 para obtener, respectivamente, el crecimiento en forma de levadura o micelio (Ruiz-Herrera y col., 1995) Los cultivos fueron centrifugados a 16000 x *g* por 10 minutos a 4 °C y el paquete celular fue congelado a -80 °C y almacenado hasta su uso.

4.2 Extracción de proteínas

Las células fueron empaquetadas por centrifugación a 8000 rpm por 10 min, realizando posteriormente cuatro lavados con Tris 10 mM y EDTA 1mM. El paquete celular obtenido fue resuspendido en 500 µL del buffer de extracción ácida (Urea 7M, Tiourea 2M, CHAPS 4% y Ácido cítrico 80 mM). Se sónico con por 1.5 min con una amplitud de 22%. Posteriormente se centrifugo a 13000 rpm por 10 min a 4 °C para recuperar el sobrenadante. Las proteínas fueron precipitadas con acetona a -20 °C durante toda la noche a -20 °C, transcurrido este tiempo se centrifugo a 13000 rpm por 10 min a 4 °C, se descarto el sobrenadante y se dejo evaporar los restos de acetona. La pastilla de proteínas fue resuspendida en el buffer de rehidratación (Urea 8M, CHAPS 2%, Ditiotreitol 1.8 mM). La concentración de proteínas fue cuantificada con el reactivo Protein Assay Dye Reagent (BioRad) de acuerdo a las instrucciones del fabricante.

4.3 Electroforesis bidimensional

Las proteínas solubilizadas fueron usadas para cargar tiras de gradiente de pH inmovilizado (IPG) de 11 cm con un intervalo de 5 a 8 (BioRad). Las tiras fueron rehidratadas por 12 horas y después fueron enfocadas en el IPGphor II (GE healthcare) con un paso previo de 150 V por 2 horas seguido por un programa con un voltaje final de 60 000 V/h. Las tiras enfocadas fueron equilibradas por 15 min en el buffer de equilibrio (Tris-HCl 50 mM, pH 8.8, Urea 6M, Glicerol 30 %, SDS 2% y Azul de bromofenol 0.002% y Ditiotreitol 1%). La separación de proteínas para la segunda dimensión fue realizada en geles de acrilamida al 12% usando la cámara de electroforesis Ruby cell (GE Healthcare) con una corriente constante de 20 mA/gel a 4°C.

4.4 Análisis de imágenes

Los geles fueron teñidos con azul de Coomasie G-250 (Bio-Rad)y digitalizados en el fotodocumentador Gel-doc (Bio-Rad). La detección de puntos y cuantificación de su volumen fue realizada en con el software Melanie 7 (GeneBio, Geneva, Switzerland). Se realizaron tres experimentos independientes para cada una de las condiciones. Los cambios en la expresión fueron considerados significativos si la media normalizada del volumen de un punto variaba al menos 1.6 veces y se confirmaba por un análisis de varianza con un nivel de significancia de $P \leq 0.05$.

4.5 Digestión en gel

Los puntos seleccionados fueron cuidadosamente cortados de los geles y lavados exhaustivamente con agua milliQ y NH_4HCO_3 25 mM. Posteriormente fueron deshidratados con acetonitrilo para remover contaminantes y desteñir completamente. Las muestras fueron diluidas con DTT 10 mM en una solución de NH_4HCO_3 25 mM, seguida de una alquilacion con iodoacetamida 55 mM. La digestión fue realizada toda la noche a 37 °C con tripsina grado secuenciación (Promega, Madison, WI, USA). Los fragmentos trípticos resultantes fueron extraídos dos veces con una solución de acetonitrilo y agua (3:2 v/v) conteniendo

0.1% de ácido trifluoroacetico. Los dos sobrenadantes fueron concentrados y los péptidos trípticos fueron desalados y concentrados a un volumen final de 5 µl con el sistema de puntas Zip-Tip C_{18} (Millipore, Billerica, MA, USA), de acurdo a los protocolos del fabricante.

4.6 Espectrometría de masas

Los análisis de espectrometría de masas fueron realizados en el equipo Synapt-HDMS (Waters Corp, Milford, MA, USA) acoplado en línea a el nano-ACQUITY-UPLC (Waters). Los péptidos fueron cargados en la pre-columna Symetry C18 (5 µm, 20 mm x 180 µm). La separación de los péptidos se realizo en la columna analítica BEH130 C18 (1.7 µm, 10 cm x 100 µm) y eluidos a 35 °C con gradiente lineal de fase móvil B (0.1% ácido formico en acetonitrilo) por 30 min con un flujo de 600 nL/min, seguido de un enjuague con 85% de fase móvil B. La columna fue nuevamente equilibrada a las condiciones iniciales por 15 minutos con la fase móvil A (0.1% ácido formico en agua). Como referencia en el spay de referencia se utilizo [Glu^1]-fibrinopeptide B, entregado por la bomba auxiliar del sistema a 200 nl/min a una concentración de 100 fmol/µl.

El RF aplicado al analizador de masas de cuádruplo fue ajustado para transmitir eficientemente los iones con una relación *m/z* de 50-3000. El espectrómetro de masa fue operado en modo V para todas las mediciones y los análisis se realizaron en modo ESI. Los datos MS/MS fueron obtenidos para más de tres cargas de iones 2^+, 3^+,4^+ detectados y obtenidos en una rampa de colisión de energía de 15 a 40 eV, la adquisición fue cambiada del modo MS a MS/MS cuando la intensidad del pico base excedía el umbral de 10 cuentas y regresaba al modo MS después de 5 s.

4.7 Búsqueda en base de datos

La interpretacion e identificación de las proteínas fue realizada con los datos de los espectros MS/MS usando el algoritmo de búsqueda MASCOT (Matrix Science, London, UK, http://www.matrixscience.com). La base de datos usada fue NCBInr (http://www.ncbi.nih.gov). Los parámetros utilizados en la búsqueda fueron:

tripsina como proteasa específica, carbamidometilacion de las cisteínas como modificaciones fijas y oxidación de la metionina como modificaciones variables. La identificación fue considerada acertada cuando se obtenía un score significativo en MASCOT con un valor de $P<0.05$. El numero de acceso del resultado dado por MASCOT se confirmo en la base de datos del Munich Information Center for Protein Sequences para *Ustilago maydis* (http://mips.helmholtz-muenchen.de/genre/proj/ustilago/). La homología de algunas proteínas fue buscada en la base de datos Pfam (http://pfam.sanger.ac.uk/.)

V. RESULTADOS

4.1 Analysis of the regulation of the *Ustilago maydis* proteome by dimorphism, pH or MAPK and GCN5 genes

(Artículo publicado en línea: Journal of Proteomics http://dx.doi.org/10.1016/j.jprot.2012.12.022)

Accepted Manuscript

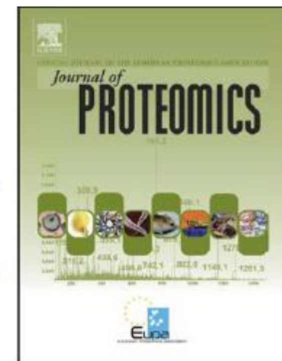

Analysis of the regulation of the *Ustilago maydis* proteome by dimorphism, pH or *MAPK* and *GCN5* genes

José L. Martínez-Salgado, Claudia G. Leon-Ramírez, Alberto Barrera Pacheco, José Ruiz-Herrera, Ana P. Barba de la Rosa

PII: S1874-3919(13)00009-2
DOI: doi: 10.1016/j.jprot.2012.12.022
Reference: JPROT 1268

To appear in: *Journal of Proteomics*

Received date: 3 August 2012
Accepted date: 30 December 2012

Please cite this article as: Martínez-Salgado José L., Leon-Ramírez Claudia G., Pacheco Alberto Barrera, Ruiz-Herrera José, de la Rosa Ana P. Barba, Analysis of the regulation of the *Ustilago maydis* proteome by dimorphism, pH or *MAPK* and *GCN5* genes, *Journal of Proteomics* (2013), doi: 10.1016/j.jprot.2012.12.022

This is a PDF file of an unedited manuscript that has been accepted for publication. As a service to our customers we are providing this early version of the manuscript. The manuscript will undergo copyediting, typesetting, and review of the resulting proof before it is published in its final form. Please note that during the production process errors may be discovered which could affect the content, and all legal disclaimers that apply to the journal pertain.

ACCEPTED MANUSCRIPT

Analysis of the regulation of the *Ustilago maydis* proteome by dimorphism, pH or *MAPK* and *GCN5* genes

José L. Martínez-Salgado[1], Claudia G. Leon-Ramírez[2], Alberto Barrera Pacheco[1], José Ruiz-Herrera[2], and Ana P. Barba de la Rosa[1*]

[1]IPICyT, Instituto Potosino de Investigación Científica y Tecnológica. Camino a La Presa San José No. 2055, Lomas 4ª Sección, 78216, San Luis Potosí, SLP, Mexico.

[2]Centro de Investigación y de Estudios Avanzados del IPN, Unidad Irapuato, Apdo. 629, 36500 Irapuato Gto., Mexico.

*We dedicates this work to the memory of Dr. G. Mendoza

Corresponding authors at: E-mail: apbarba@ipicyt.edu.mx (A. P. Barba de la Rosa) or jruiz@ira.cinvestav.mx (J. Ruíz-Herrera).

ACCEPTED MANUSCRIPT

ACCEPTED MANUSCRIPT

ABSTRACT

Ustilago maydis is a dimorphic corn pathogenic basidiomycota whose haploid cells grow in yeast form at pH 7, while at pH 3 they grow in the mycelial form. Two-dimensional gel electrophoresis (2-DE) coupled with LC-ESI/MS-MS was used to analyze the differential accumulation of proteins in yeast against mycelial morphologies. 2-DE maps were obtained in the pH range of 5-8 and 404 total protein spots were separated. From these, 43 were differentially accumulated when comparing strains FB2*wt*, constitutive yeast CL211, and constitutive mycelial GP25 growing at pH 7 against pH 3. Differentially accumulated proteins in response to pH are related with defense against reactive oxygen species or toxic compounds. Up-accumulation of CipC and down-accumulation of Hmp1 were specifically related with mycelial growth. Changes in proteins that were affected by mutation in the gene encoding the adaptor of a MAPK pathway (CL211 strain) were UM521* and transcription factors Btf3, Sol1 and Sti1. Mutation of *GCN5* (GP25 strain) affected the accumulation of Rps19-ribosomal protein, Mge1-heath shock protein, and Lpd1-dihydrolipoamide dehydrogenase. Our results complement the information about the genes and proteins related with the dimorphic transition in *U. maydis* and changes in proteins affected by mutations in a *MAPK* pathway and *GCN5* gene.

Keywords: constitutive mutants; dimorphism; proteomics; pH; two-dimensional gel electrophoresis; *Ustilago maydis.*

ACCEPTED MANUSCRIPT

Introduction

Ustilago maydis is a pathogenic Basidiomycota fungus that causes common smut in maize (*Zea mays*) and its probable ancestor, *Zea mays* subsp. *parviglumis* [1]. *U. maydis* exhibits a dimorphic switch from yeast to filamentous growth in response to mating interactions and environmental conditions. Haploid cells can form filaments *in vitro* in response to acidic pH [2], or use of fatty acids as carbon source [3]. In nature, the yeast form corresponds to the saprophytic stage of the life cycle, and exists as haploid cells that divide by budding, whereas the filamentous form is the product of mating of sexually compatible yeasts, and corresponds to the dikaryotic and pathogenic stage.

The genome-wide analysis of *U. maydis* annotated at the Munich Center for Protein Sequence (MIPS) (http://mips.gsf.de/genre/proj/ustilago/), has revealed that *U. maydis* is more closely related to humans than to budding yeast, and numerous proteins are shared only by *U. maydis* and *Homo sapiens* [4]. The reported genome also has opened new fields of research on the molecular bases of the dimorphic yeast-to mycelium transition studies. SSH and SAGE libraries have been used for the identification of up-and down regulated genes in filamentous cells [5-7]. However, not all changes in the expression level are necessarily the reflection of alterations occurring at the transcriptional level. Accordingly analyses at the level of protein composition of both forms are necessary for our understanding of the dimorphic phenomenon.

Two-dimensional polyacrylamide gel electrophoresis (2-DE) is a tool for the analysis of complex protein mixtures and for examination of the levels of protein expression in a tissue or cell type at different stages, conditions or treatments. This technique has been

ACCEPTED MANUSCRIPT

used in the studies of changes in protein expression during the dimorphic transition of different fungi, including *Candida albicans* [8,9], *Penicillium marneffei* [10], and *Candida glabrata* [11]. Also, the proteome reference map for *U. maydis* has been reported, as well the dimorphic transition induced by two independent regimes; either by overexpression of the bW2/bE1-heterodimer or by overexpression of the small GTP binding protein Rac1 [12]. However, the ability to obtain mycelial growth both in liquid and solid media [2] has opened the possibility to analyze *in vitro* the protein changes involved in the yeast-to-mycelium transition.

As indicated above, *U. maydis* grows in a yeast-like form when the initial pH of the medium is close to neutrality, whereas at pH 3 mycelial forms are obtained [2]. In addition, monomorphic mutants such as the CL211 constitutive yeast deleted in a gene coding for a member of the MAPK family [13] and GP25 constitutive mycelium mutated in the gene encoding the histone acetyl transferase *GNC5* [González-Prieto and Ruíz-Herrera, unpublished] are useful tools for search the factors directly involved in the morphological transition process. The aim of this work was to use the proteomics tools to analyze the changes in proteins related to *U. maydis* FB2 wild type dimorphic transition induced by pH, and controlled by *UBC2* [13] and *GCN5*.

2. Materials and methods

2.1. Strains and growth conditions

The strains used in this study were: FB2*wt* (*a2b2*, wild type) [14], CL211 [*a2b2myc*$^{-}$; a yeast constitutive mutant reported by Martínez-Espinoza et al. [13], and GP25 (*a2b2*

ACCEPTED MANUSCRIPT

gcn5::hyg, mycelium constitutive mutant [González-Prieto and Ruíz-Herrera, unpublished data] of *U. maydis*.

Strains were grown for 18 to 20 h in liquid complex medium (CM) [15]. The cells were recovered by centrifugation (16000 x *g*), washed twice with sterile distilled water and suspended in the original volume of sterile distilled water. The cell suspension was shaken at 28 °C for about 3 h, until most cells appeared unbudded. They were recovered by centrifugation, washed, suspended in sterile distilled water and maintained at 4 °C for not more than 48 h. These cell suspensions were used as experimental inoculum. Cell suspensions ($5x10^6$ cells ml^{-1}) were used to inoculate synthetic medium (MM) [15] maintained at 30 °C. The cultures were then incubated at 28 °C on a shaker (200 rpm) in media with an initial pH of 7.0 where the FB2*wt* strain grew as a homogeneous population of budding yeast-like cells. When the initial pH of the medium was adjusted to 3.0, almost the whole population grew in the form of mycelium. The CL211 strain grew at both pH values as budding yeast-like cells, whereas GP25 cells maintained the mycelial form at both pH values.

2.2. Light microscopy

Cells were stained with cotton blue for observation by bright field microscopy (Leica, DMRB).

2.3. Protein extraction

Cultures were centrifuged at 16000 x *g* for 10 min at 4 ºC and the cells were suspended in 500 µl of extraction acid buffer (7 M urea, 2 M thiourea, 4% (w/v) CHAPS, and 80 mM citric acid at pH 4). The cells were sonicated on ice for 1.5 min with intervals of 10 s.

ACCEPTED MANUSCRIPT

ACCEPTED MANUSCRIPT

Cells debris were removed by centrifugation at 16000 x *g* for 10 min at 4ºC [16]. The supernatant was collected and the proteins were precipitated with cold acetone. The protein pellets were solubilized in sample rehydration buffer (8M urea, 2% (w/v) CHAPS, 1.8 mM dithiothreitol, 0.5% Pharmalite 4-7 (GE Healthcare Bioscience, Piscataway, NJ; USA), and 0.002% bromophenol blue. Protein concentration was estimated using the dye-binding assay according to the manufacturer´s instructions (Bio-Rad Laboratories, Hercules, CA).

2.4. 2-DE and image analysis

Proteins solubilized in rehydration buffer were used to rehydrate 11 cm linear immobilized gradient strips (Bio-Rad) with a pH gradient from 5 to 8. Strips were rehydrated for 12 h and then focused with a pre-step of 100-150 V for 2 h in the IPGphor II (GE Healthcare) to a final 60,000 V/h. Focused strips were equilibrated for 15 min in a buffer containing 50 mM Tris-HCl, pH 8.8, 6 M urea, 30% (v/v) glycerol, 2% (w/v) SDS, 0.002% (w/v) bromophenol blue and 1% (w/v) dithiothreitol. Protein separation in the second dimension was performed in 12% SDS-PAGE using a Ruby cell (GE Healthcare). Proteins were resolved at a constant current of 20 mA/gel at 4°C.

Proteins were visualized following staining with Coomasie Brillant Blue G-250 (Bio-Rad) and gels were digitalized in a Gel-doc (Bio-Rad). Spot detection and volume quantitation were carried out with Melanie 7 (GeneBio, Geneva, Switzerland). At least three independent experiments for each growth conditions were performed. Changes on protein expression were considered significant if the mean normalized spot volume varied at least 1.6-fold and confirmed by analysis of variance at a significant level of $P \leq 0.05$.

ACCEPTED MANUSCRIPT

ACCEPTED MANUSCRIPT

2.5. In-gel digestion and MS

Selected spots were carefully excised from 2-DE gels and were washed successively with ultrapure water and 25 mM NH_4HCO_3. Gel pieces were dehydrated with acetonitrile (ACN) to remove contaminants and distain completely. Samples were reduced with 10 mM DTT in 25 mM NH_4HCO_3 followed by protein alkylation with 55 mM iodoacetamide. Digestion was carried out overnight at 37 °C with sequencing grade trypsin (Promega, Madison, WI, USA). The resulting tryptic fragments were extracted twice with ACN:water (3:2 v/v) containing 0.1% trifluoroacetic acid. The pooled supernatants were concentrated and the tryptic peptides were desalted and concentrated to a final volume of 5 μL with Zip-Tip C_{18} (Millipore, Billerica, MA, USA), according to the manufacturer´s protocol.

Mass spectrometric analysis was carried out on a SYNAPT-HDMS (Waters Corp, Milford, MA, USA) coupled online to the nano-ACQUITY-UPLC (Waters). The peptides were loaded onto a Symmetry C18 pre-column (5 μm, 20 mm x 180 μm). Peptide separation was carried out on a BEH130 C18 (1.7 μm, 10 cm x 100 μm) analytical column (Waters) and eluted at 35 °C with a linear gradient of 3-50% mobile phase B (0.1% formic acid in ACN) over 30 min at a flow rate of 600 nL/min, followed by a 3 min rinse with 85% of mobile phase B. The column was re-equilibrated at initial conditions for 15 min with mobile phase A (0.1% formic acid in water). The lock mass compound, [Glu^1]-fibrinopeptide B, was delivered by the auxiliary pump of the UPLC system at 200 nl/min at a concentration of 100 fmol/μL, to the reference sprayer of the NanoLock Spray source of the mass spectrometer. Samples were analyzed at least by duplicate.

ACCEPTED MANUSCRIPT

The RF applied to the quadrupole mass analyzer was adjusted in such a way that ions from *m/z* 50-3000 were efficiently transmitted. For all measurements the mass spectrometer was operated in V-mode, and all analyses were carried out in positive mode ESI. The data were post-acquisition lock mass corrected using the doubly protonated mono-isotopic ion of [Glu^{1}]-fibrinopeptide B. The reference sprayer was sampled every 30 s. For LC-MS/MS Data Dependent Analyses, MS survey scans of 1 s duration in continuum mode were acquired. MS/MS data were obtained for up three ions of charge 2^+, 3^+, 4^+ detected in the survey scan. MS/MS was obtained at a scan rate of 1 s and a collision energy ramp from 15 to 40 eV. Acquisition was switched from MS to MS/MS mode when the base peak intensity exceeded a threshold of 10 counts, and returned to the MS mode after 5 s.

2.6. Database searching

Data interpretation and protein identification were performed on the MS/MS spectra datasets using the MASCOT search algorithm (Matrix Science, London, UK, http://www.matrixscience.com). Searches were conducted using the NCBInr database (http://www.ncbi.nih.gov) and MUMDB (http://mips.gsf.de/genre/proj/Ustilago). Trypsin was used as the specific protease and one missed cleavage was allowed. The mass tolerances were fixed at 0.6 Da for the precursor and 0.3 Da for the fragment ion masses. Carbamidomethyl of Cys was set as fixed modification and deamidation of Asn and Gln, propionamide Cys, and oxidation on Met were specified as variable modifications. Identifications were considered successful when a significant MASCOT score was obtained and indicating the identity or extensive homology at $P<0.05$. Protein

ACCEPTED MANUSCRIPT

homologies were searched at Pfam protein database [17] located at http://pfam.sanger.ac.uk/.

3. Results

3.1. Morphology of U. maydis when grows in synthetic media at pH 7 or *pH 3*

Filament formation in *U. maydis*, a dimorphic plant pathogenic fungus, is characterized by highly polarized tip growth and is critical for pathogenic development. We have the ability to grow *U. maydis* FB2*wt* in liquid synthetic media and change its morphology by changing the media pH; whereas at pH 7.0 the fungus grows in the yeast form (Fig. 1A); at pH 3 it grows in the mycelial form (Fig. 1B). The mutants CL211and GP25, which have respectively a yeast and mycelial constitutive morphology, are shown in Fig. 1(C-D) and Fig. 1(E-F).

3.2. Identification of differentially accumulated proteins in U. maydis FB2wt and constitutive mutants CL211 and GP25

To identify changes in the protein expression associated with dimorphism of *U. maydis*, the 2-DE protein patterns of the FB2*wt*, and mutants CL211 and GP25 were compared. Although a previous electrophoretic analysis of the *U. maydis* proteome was carried out at pH ranges of 3-10 and 4-7 [12], we have used an acidic protein extraction protocol that improves the protein yield, and as a result the 2-DE pattern in the range of pH 3-10 (Fig. S1A) showed that the most representative pH for *U. maydis* proteome ranged from 5 to 8 (Fig. S1B). Fig. S2 shows a representative 2-DE map for each strain when grows in media at pH 7 or pH 3. A total of 404 protein spots were reproducibly detected, this is a higher amount of spots detected without any overlap than those reported previously

ACCEPTED MANUSCRIPT

[12]. We have used a regulation factor of 1.6 in a standardized average spot volume ratio, as calculated being significant, as a result, 43 protein spots showed significant differences among different strains (Table 1, Fig. 2). Zoomed images on Fig. 2 and Fig. S3 show examples of up- or down- accumulated protein spots. Some proteins, such as UM00961, were found in two different spot with slightly p*I* differences (6.5 and 6.3), indicating that these proteins were modified post-translationally (PTMs).

3.3. Differentially accumulated proteins when cells were grown at pH 7 against pH 3

Differentially accumulated proteins were obtained when comparing protein profiles of each strain grown at pH 7 against pH 3. The up- and down-accumulated proteins, specific of each strain or those that were found in two or three of them, are shown in Venn diagrams on Fig. 3A and 3B, respectively. Under this analysis, proteins that were found in all strains (intersection area) reflect the *U. maydis* proteins regulated by change of pH. These proteins, such as peroxisomal membrane proteins and aldo-keto-reductase are related with the defense against reactive oxygen species or toxic compounds.

A second group of Venn diagram was constructed in which we incorporated the following comparisons: *a*) FB2*wt* proteins regulated at pH 3 (mycelium) with those regulated pH 7 (yeast), *b*) FB2*wt* proteins regulated at pH 3 (mycelium) with those from CL211 regulated at pH 3 (yeast), and *c*) FB2*wt* proteins regulated at pH 7 (yeast) with those from GP25 regulated at pH 7 (mycelium). The proteins that were located at the intersection corresponded to those proteins specific of the dimorphic transition. The up-accumulated (mycelial) or down-accumulated (yeast) proteins are shown in Fig. 4A and 4B, respectively. The up-accumulation of UM03284 or the CipC (shown in zoomed

ACCEPTED MANUSCRIPT

image in Fig. 2) protein has been reported before, but our proteomic approach also shows the down-accumulation of a second protein, the UM00496, identified as the cruciform DNA recognition protein Hmp1 (shown in zoomed image in Fig. 2).

4. Discussion

4.1. Differentially accumulated proteins in response to pH

FB2*wt* and mutants CL211 and GP25 shared the up-accumulation of two proteins when pH changes from 7 to 3 (Fig. 3A). Those corresponded to spot 20 (UM02947, peroxisomal membrane protein) and spot 113 (UM06344, 2-methylcitrate dehydratase). Peroxisomes are single membrane-enclosed organelles of eukaryotic cells harboring enzymes involved in lipid metabolism and defense systems for *in situ* scavenging of peroxides and reactive oxygen species [19,20]. Peroxisomal proteins have been also found in Woronin bodies of filamentous fungi that function as a plug for the sealing of septal pores upon injury of the syncytium. Fungal and plant peroxisomes have been also involved in the production of antibiotics, toxins, and signaling molecules [21].

The functional methylcitrate cycle is essential for the efficient removal of propionyl-CoA that is a potentially toxic metabolite inhibitor of both primary and secondary metabolism. It has been reported that in plant-pathogenic fungi, such as *Fusarium* species, it is possible that propionyl-CoA-generating carbon sources such as odd chain fatty acids or amino acids are consumed during plant infection; this pathway might play an important role during pathogenesis and therefore constitute a novel antifungal target [22].

Proteins that were found to be down-accumulated in response to the change in pH from pH 7 to pH 3 (Fig. 3B) were one isoform of the hypothetical protein UM00961*

ACCEPTED MANUSCRIPT

ACCEPTED MANUSCRIPT

(spot 48). UM01209 (spot 121), that corresponded to mitochondrial Ssc1 that belongs to the Hsp70 protein family. Ssc1 is the most abundant constitutively expressed protein being essential for *S.cerevisiae* cells viability [23,24]. Another down-accumulated protein was UM06052 (spot 126) corresponding to an aldo/keto reductase. Most aldo-keto reductases (Akrs) catalyze the first step of the polyol pathway via the conversion of glucose into sorbitol. In humans, this pathway likely contributes to tissue pathogenesis associated with diabetes mellitus. In *S. cerevisiae* disruption of at least three Akr genes results in a heat shock phenotype and slow growth in inositol-deficient culture medium [25]. The last protein, UM02703 (spot 128) was related with the fructose 1,6-bisphosphate, enzyme that catalyzes the reversible aldol condensation of dihydroxyacetone phosphate (DHAP) and glyceraldehyde 3-phosphate (GAP) in glycolysis, gluconeogenesis, and Calvin cycle [26].

Changes in pH affect the expression of different proteins depending on *U. maydis* morphology. In relation to yeast morphology (FB2*wt*, pH 7 and CL211), it was found the down accumulation of UM02158 and UM00594 (Fig. 3). UM02158 has homology with the members of the peptidase family M20, belonging to the metallopeptidase H family. These have diverse functions throughout all kingdoms of life, ranging from a general role in the hydrolysis of late products of protein degradation to specific biochemical functions in protein maturation, tissue repair, and cell-cycle control [27]. UM00594 (spot 130) was homologous to the dihydrolipoamide S-acetyltransferase (E2) subunit of the maize mitochondrial pyruvate dehydrogenase complex [28].

When *U. maydis* grows in the form of mycelium (FB2*wt* pH 3 and GP25), two protein spots were found up-accumulated, the first one corresponded to Lys12-homo-isocitrate

ACCEPTED MANUSCRIPT

dehydrogenase UM04873 (spot 89). This protein is involved in the α-aminoadipate pathway of lysine biosynthesis in some bacteria and higher fungi. This pathway is unique for human and plant pathogens, therefore enzymes involved in this pathway are considered to be a potential target for new anti-fungal drugs [29]. The second up-accumulated protein related with mycelial morphology corresponded to another isoform of UM06404.

Among the down-accumulated proteins in the mycelial form of FB2*wt* and GP25 was UM05993 (spot 105), identified as the Mas1 mitochondrial processing peptidase. Mas1 is a metallopeptidase that cleaves off most of the N-terminal pre-sequences from precursor proteins destined for the mitochondrial matrix or the intermediate and inner membrane spaces [30]. Another protein was F_1F_0-ATPase complex (spot 108, UM03191) that plays a central role in oxidative phosphorylation and thus respiration in all aerobic organisms [31]. Lack of ATP synthase also affects the morphology of mitochondria, which are deprived of cristae [32]. It is well known that several glucohydrolases appeared during dimorphic transition, but it has not been reported the presence of alpha-amylases [33]. In this work we have found the down-accumulation of spot 131 (UM02300) related to one alpha-amylase.

4.2. Differentially accumulated proteins specifically regulated during dimorphism

Results of the analysis of protein expression in the three *U. maydis* strains where the common factor was dimorphism are represented in Venn diagrams (Fig. 4A and 4B). Only two proteins were found related to dimorphism, the up-accumulated UM03284 (Fig. 4A) and the down-raccumulated UM00496 (Fig. 4B). The protein spot 125 (UM03284), identified as one conserved hypothetical protein (shown in zoomed image

ACCEPTED MANUSCRIPT

in Fig. 2) has been described as the homologue of CipC. This is a protein that was also over-accumulated under conditions of nitrogen starvation in *U. maydis* [1,12]. Böhmer et al. [12] described that in the mycelial form CipC could be involved in the production of specific components needed for the synthesis of the hyphal cell wall.

The down-accumulated protein in the mycelial form of FB2*wt* was UM00496 (UM1130), identified as the cruciform DNA recognition protein Hmp1 (shown in zoomed image in Fig. 2). The cruciform DNA binding activity was found in extracts of *U. maydis* [34]. The *Hmp1* sequence analysis showed that *U. maydis* Hmp represents a novel class of proteins that recognize DNA secondary structures [35], and further work should be done in order to clarify its function during dimorphic transition.

4.3. Differentially accumulated proteins in FB2wt when comparing the yeast against mycelial form: proteins important for morphology changes

Protein spots corresponding to the UM04507, UM05662, and one isoform of UM06404** were found up-accumulated only in wild strain FB2*wt* when cells changes from yeast to mycelium (Fig. 3A). The UM04507 (spot 19) corresponded to the Tpm2-tropomyosin isoform 2, an important actin filament stabilizing protein [36]. Tpm2 has been found more abundant in the mycelial morphology of *Candida albicans*, and related with the polarized cell growth [9]. Spot 54 (UM05662) was identified as the voltage-dependent anion-selective channel (Vdac) known as the mitochondrial porin. Vdac is the major protein of the outer mitochondrial membrane of eukaryotes that behaves as a general diffusion pore for small hydrophilic molecules (*e.g.*, Ca^{2+}, and respiratory substrates) including adenine nucleotides [37,38].

ACCEPTED MANUSCRIPT

Several isoforms of spot 42 (UM06404) were identified, one was over-accumulated only in FB2*wt*. UM06404 was identified as a thioredoxin peroxidase. Thioredoxin belongs to an important conserved system for protection against oxidative stress by reducing peroxides such as H_2O_2 to harmless products [39]. The modification of this protein could be important for the mycelial form.

The down-accumulated proteins were the aldo-keto reductase yakc [NADP+] (UM03006, zoomed image shown in Fig. 4D) and the mitochondrial Ilv5-ketol-acid reducotoisomerase (UM04741, spot 80). Ilv5-ketol acid is a bifunctional yeast mitochondrial enzyme required for branched chain amino acid biosynthesis and for the stability of mitochondrial DNA (mtDNA) and its parsing into nucleoids [40]. Mitochondrial nucleoids in *S. cerevisiae* are dynamic structures that are remodeled in response to metabolic cues [41,42]. A second isoform of UM00961 (spot 50) was also observed down-accumulated in the mycelial morphology as well as by the action of a pH change, as described above.

The alpha chain of the H^+-transporting ATP synthase (UM05379, spot 113) is a protein known as vacuolar (H+)-ATPase (V-ATPase) and occurs as a multi-protein membrane-bound enzymatic complex present in almost all types of eukaryotic cells. The enzyme is an ATP-driven proton pump, acting as a molecular motor, which is responsible for the acidification of intracellular compartments in eukaryotic cells. Acidification of intracellular compartments of vacuoles is essential for various cellular processes including ligand-receptor dissociation and protein [43,44].

4.4. Differentially accumulated proteins in CL211 constitutive yeast and GP25 constitutive mycelial mutant

ACCEPTED MANUSCRIPT

ACCEPTED MANUSCRIPT

Proteins that change only in CL211 and GP25 as a result of the corresponding mutations represent proteins related with cell metabolism such as UM06404** (one isoform of thioredoxin, spot 42), UM02801, UM00674, UM00787, UM00635, UM05754, and UM05969 (Fig. 3B).

The NADP-glutamate dehydrogenase (UM02801, spot 101), is encoded in *S. cerevisiae* by *Gdh1* and *Gdh3*, both are enzymes responsible to synthesize glutamate from α-ketoglutarate, while an NAD-dependent enzyme, encoded by *Gdh2* catalyzes the reverse reaction. *In vivo* studies have shown that Gdh1p is the primary Gdh enzyme, and Gdh2p and Gdh3p play evident roles during aerobic glutamate metabolism [45]. Fba1 fructose-bisphosphate aldolase (UM00674, spot 79) catalyzes the reversible aldol condensation of dihydroxyacetone phosphate (Dhap) and glyceraldehyde 3-phosphate (Gap) in glycolysis, gluconeogenesis, and the Calvin cycle [26]. Fum1, fumarate hydratase (UM00787, spot 103) has been suggested to participate as a scavenger of fumarate from the urea cycle and in the catabolism of amino acids. In *S. cerevisiae*, *Fum1* gene is expressed as a single translation product, which is distributed between the cytosol and the mitochondria via a unique mechanism. In mitochondria Fum is involved in generating energy for the cell through the TCA cycle. When Fum is absent, its function in DNA repair can be substituted by high concentrations of one of the enzyme´s products, fumaric acid. It has been reported that Fum deficiency leads to cancer because there is not enough fumaric acid in the nucleus to stimulate repair of DNA double-strand breaks; the persistence of these breaks is believed to provoke cancer [46].

ACCEPTED MANUSCRIPT

The conserved hypothetical protein UM00635 (spot 118) was identified as a mitochondrial protein named mitofilin of unknown function. Mitofilin proteins control the mitochondrial cristae morphology and are found enriched in the narrow space between the inner boundary and the outer membranes, where it forms a homotypic interaction and assembles into a large multimeric protein complex. It has been reported that the down-regulation of mitofilin in HeLa cells, by using specific small interfering RNA, leads to decreased cell proliferation and increased apoptosis, suggesting abnormal mitochondrial function [47]. The alpha chain precursor of the electron transfer flavoprotein Etf (UM05754, spot 77), is in mammals a heterodimeric protein composed of two subunits, α and β, that is responsible for the oxidation of at least nine mitochondrial matrix flavoprotein dehydrogenases, including four chain-length-specific acyl CoA dehydrogenases involved in straight-chain fatty acid β–oxidation and sarcosine and dimethylglycine dehydrogenases, which are involved in choline metabolism [48]. UM05969 (spot 70) belongs to a member of the short-chain dehydrogenases/reductases family known as Sdr, most of which are known to be NAD- or NADP-dependent oxidoreductases. Sdr superfamily forms a well-established enzyme family of oxidoreductases distinct from functionally related enzyme families such as medium-chain dehydrogenases/reductases (Mdr) or aldo-keto reductases [49]. Sdrs act on a wide spectrum of substrates, ranging from steroids, alchohols, sugars, and aromatic compounds to xenobiotics [50].

4.4.1. Differentially accumulated proteins in CL211: effect of gene mutation encoding the adaptor of the MAPK pathway

ACCEPTED MANUSCRIPT

CL211 strain has a mycelial minus phenotype (*myc*-) due to mutation in the gene encoding the adaptor of the MAPK pathway [13]. It was observed that deletion of MAPK in *Aspergillus nidulans* affects severely the developmental process including sexual differentiation [51]. Our proteomic analysis showed that protein spot 32 corresponding to the GTP-binding nuclear protein Ran (UM521*) was found up-accumulated in CL211 (Fig. S3A). Ran-GTPases influence many cellular functions including nucleocytoplasmic transport, nuclear envelope reformation after mitosis in animal cells, and nuclear structure in fission and budding yeast [52,53]. UM05339 (spot 49), was also over-accumulated (Fig. 3B). This spot was related with the 2,3-bisphosphoglycerate-dependent phosphoglycerate mutase, an enzyme that is involved during the interconversion of 3-phosphoglycerate and 2-phosphoglycerate [54].

The down-accumulation of proteins affected by MAPK mutation where UM03074, UM02360, UM03539, UM01712, UM03811 UM02621, and UM02057 (Fig. S3B). UM03074 (spot 141) corresponded to Btf3a transcription factor. Btf3 was originally identified in HeLa cell extracts as one of the basal transcription factors required for accurate transcription from class II promoters [55]. UM02360 (spot 35) has homology with the ATP_sub_h, a component of the yeast mitochondrial F_1F_0 ATP synthase that is essential for the correct assembly and functioning of this enzyme [56].

UM03539 (spot 69) has homology with dienelactone hydrolase which is a member of an a/b-hydrolase fold family which have diverse catalytic functions. Dienelactone (DLH) is an enzyme used by bacteria and fungi to degrade aromatic compounds such as dienelactone to maleylacetate [57]. The hypothetical protein UM01712 (spot 63) has homology with amphiphysin, a protein that is found in the Bar (Bin-Amphiphysin-Rvs)

ACCEPTED MANUSCRIPT

domain-containing proteins, that are highly conserved protein dimerization domains that occur in many proteins involved in the membrane dynamics of the cell. The Bar domain is banana shaped and binds to membrane via its concave face. It is capable of sensing membrane curvature by binding preferentially to curve membranes [58].

UM03811 protein (spot 65) was identified as Sol1. In *C. albicans* it has been described that Sol1 is a substrate of Cdc4, which is essential for cell proliferation. Deletion of *SOL1* has indicated a role for this gene in *C. albicans* morphogenesis [59]. UM02621 (spot 129) was related to the Agx1-alanine-glyoxylate transaminase, an enzyme involved in the glyoxylate pathway, and of glycine and serine biosynthesis from tricarboxylic acid-cycle intermediates in *S. cereviceae* [60].

Another down-accumulated protein was spot 119 (UM02057) related with Sti1 (Sti1 in *S. cerevisiae*, Hop in mammalian cells) is a stress inducible co-chaperone that functions as an adaptor protein that simultaneously binds to Hsp79 and Hsp90 through separate tetraticopeptides repeat (TPR) to transfer client proteins from Hsp70 to Hsp90 [61].

4.4.2. Differentially expressed proteins in GP25: effect of histone deacetylation mutation

The differentially accumulated proteins affected by histone deacetylation mutation on GP25 strain are shown in Fig. S4A and S4B. Up-accumulated proteins were UM03074 and UM04662 and down-accumulated were UM03493 and UM02461. UM03074 corresponded to BTF3a transcription factor that was found down-accumulated in CL211 but in GP25 was up-accumulated. Spot 1 (UM04662) was found only in the hypha constitutive GP25 mutant. This spot corresponded to the Rps19B-ribosomal protein S19, a 16-kDa protein found mainly as a component of the ribosomal 40S subunit. Like other Rps, Rps19 is translocated from the cytoplasm to the nucleus where it participates

ACCEPTED MANUSCRIPT

in ribosome biogenesis. In *S. cerevisiae* its absence is associated with abnormal rRNA cleavage and defective 40S biogenesis [62,63].

Among the down-accumulated proteins found only in the mycelium constitutive mutant GP25 were the spot 34 and spot 123. The first (UM03493) corresponded to the Mge1-heat shock protein, known as GrpE in bacteria. Mge1p is a nucleotide exchanger that stimulates ATP hydrolysis by the mitochondrial protein Ssc1p (DnaK). Mge1p cooperates with Ssc1p and Mdj1p (DnaJ) to unfold other proteins in order to facilitate their import into mitochondria and maintaining protein homeostasis [64,65]. The second corresponded to the multifunctional protein LPD1-dihydrolipoamide dehydrogenase (UM02461) characterized as the E3 component of the pyruvate dehydrogenase and α-ketoglutarate dehydrogenase complexes. Lpd1 was identified in *C. albicans* on a two dimensional polyacrylamide gel-electrophoresis as a hypha-specific proteins and in a homozygotic *lpd1/lpd1* mutant it was shown to be required for filamentous growth [66].

5. Conclusions

In this work we have improved the protein extraction method to analyze the total soluble proteins of *U. maydis*. Under the present protocol of extraction the 2-DE profile was obtained in a pH range of 5 to 8. These modifications allowed improving the separation of proteins during the electrophoresis, eliminating the superimposition of protein spots and provided complementary data of the differential proteins existing in the yeast and mycelia stages of the fungus.

Specific proteins related to dimorphism were found when proteins affected by pH changes in the medium were eliminated; then dimorphism was related with the up-accumulation of CipC and down-accumulation of Hmp1. In mycelial morphology it was

ACCEPTED MANUSCRIPT

found the differential accumulation of TPM2, thioredoxin, Vdca, Ilv5, and Akr. In the yeast constitutive mutant (CL211) whose mutation affects the *MAPK* pathway, several transcription factors such as Btfa3, Bar, Sol, Sti1, and dienelactone were found down-accumulated, while RAN-GTPase was up-accumulated. In the mycelium constitutive mutant GP25 obtained by *GNC5* disruption, the Rps19B was up-accumulated. Down-accumulation of proteins in the mutants, means that they are up-regulated by the missing gene, and up-accumulation of proteins in the mutants means that they are down-regulated by the corresponding gene. The decrease in the abundance of enzymes of glycolysis and Krebs pathways in mutants CL211 and GP25, such as short-chain dehydrogenase/reductases, the electron transfer, Fum1 and NADP-glutamate dehydrogenase could be related with pleiotropic effects of gene mutation. It is also well known that changes from respiratory to fermentative metabolism are part of the mechanisms related with the mycelial-to-yeast transition. Our proteomics data are in good agreement with this concept since we have found decrease in abundance in proteins related to respiratory process such as ATPaseF_1-F_0, and H^{+}-transport ATPase. Also we have found a decrease in proteins such as amphysisin and mitofilin related with mitochondrial membrane dynamics. Future work should be done in order to determine the regulation of different isoforms of the thioredoxin peroxidase (UM06404) and the hypothetical protein (UM00961) with no homology found in databases but which appear to be essential for the yeast morphology.

Acknowledgments

JL Martínez-Salgado thanks to CONACYT-Mexico for his PhD fellowship No. 175592. We thank to CONACyT Grant 56787 (Laboratory for Nanoscience and Nanotechnology

ACCEPTED MANUSCRIPT

Research-LINAN), and grants to JRH for partial support of this work. Thanks are given to Adán T. Morales-Vargas for fruitful discussions.

Appendix A. Supplementary data

Table S1.

Figure S1.

Figure S2.

Figure S3.

Figure S4.

Figure S5.

ACCEPTED MANUSCRIPT

References

[1] Bölker M. *Ustilago maydis* – a valuable model system for the study of fungal dimorphysm and virulence. Microbiol 2001;147:1395-1401.

[2] Ruíz-Herrera J, Leon CG, Guevara L, Cárabez A. Yeast-mycelial dimorphism of haploid and diploid strains of *Ustilago maydis*, Microbiol 1995;141: 696-703.

[3] Klose J, Moniz De Sá M, Kronstad JW. Lipid-induced filamentous growth in *Ustilago maydis*. Mol Microbiol 2004;52:823-835.

[4] Steinberg G, Perez-Martin J. *Ustilago maydis*, a new fungal model system for cell biology. Trends Cell Biol 2007;18:61-67.

[5] Andrews DL, García-Pedrajas MD, Gold SE. Fungal dimorphism regulated gene expression in *Ustilago maydis*: I. Filament up-regulated genes. Mol Plant Pathol 2004;5:281-293.

ACCEPTED MANUSCRIPT

[6] García-Pedrajas MD, Gold SE. Fungal dimorphism regulated gene expression in *Ustilago maydis*: II. Filament down-regulated genes. Mol Plant Pathol 2004;5:395-307.

[7] Larraya LM, Boyce KJ, so A, Steen BR, Jones S, Marra M, Kronstad JW. Serial analysis of gene expression reveals conserved links between protein kinase A, ribosome biogenesis, and phosphate metabolism in *Ustilago maydis*. Eukaryot Cell 2005;4:2029-2043.

[8] Hernandez R, Nombela C, Diez-Orejas R, Gil C. Two dimensional reference map of *Candida albicans* hyphal forms. Proteomics 2004;4:374-382.

[9] Monteoliva L, Martinez-Lopez R, Pitarch A, Hernandez ML, Serna A, Nombela C, Albar JP, Gil C. Quantitative proteome and acidic subproteome profiling of *Candida albicans* yeast-to-hypha transition. J Proteome Res 2011;10:502-517.

[10] Chandler JM, Treece ER, Trenary HR, Brenneman JL, Flickner TJ, Frommelt JL, Oo ZM, Patterson MM, Rundle WT, Valle OV, Kim TD, Walker GR, Cooper CR Jr. 2008. Protein profiling of the dimorphic, pathogenic fungus, *Penicillum marneffei*. Proteome Sci 2008;6:17.

[11] Schmidt P, Walker J, Selway L, Stead D, Yin Z, Enjalbert B, Weir M, Brown AJP. Proteomic analysis of the pH response in the fungal pathogen *Candida glabrata*. Proteomics 2008, 8:534-544.

[12] Böhmer M, Colby T, Böhmer C,Bräutigam A, Schmidt J, Bölker M. Proteomic analysis of dimorphic transition in the phytopathogenic fungus *Ustilago maydis*. Proteomics 2007;7:675-685.

[13] Martínez-Espinoza AD, León C, Elizarraraz G, Ruiz-Herrera J. Monomorphic nonpathogenic mutants of *Ustilago maydis*. Phtyopathol 1997;87:259-265.

[14] Banuett F, Horskowitz I. Morphological transition in the life cycle of *Ustilago maydis* and their genetic control by the a and b loci. Exp Mycol 1994;18:247-266.

[15] Holliday R. The genetics of *Ustilago maydis*. Genet Res 1961;2:204-230.

[16] Herbert BR, Grinyer J, McCarthy JT, Isaacs M, Harry EJ, Nevalainen H, Traini MD, Hunt S, Schulz B, Laver M, Goodall AR, Packer J, Harry JL, Williams KL. Improved 2-DE of microorganisms after acidic extraction. Electrophoresis 2006;27:1630-1640.

ACCEPTED MANUSCRIPT

[17] Finn RD, Mistry J, Tate J, Coggill P, Heger A, Pollington JE, Gavin OL, Gunasekaran P, Ceric G, Forslund K, Holm L, Sonnhammer EL, Eddy SR, Bateman A. The Pfam protein families databases. Nucleic Acids Res 2010;38:D211-22.

[18] Morales-Vargas A, Dominguez A, Ruiz-Herrera J. Identification of dimorphism-involved genes of *Yarrowia lipolytica* by means of microarray analysis. Research in Microbiology (2012), doi:10.1016/j.resmic.2012.03.002

[19] Ma C, Agrawal, G, Subramani S. Peroxisome assembly: matrix and membrane protein biogenesis. J Cell Biol 2011;193:7-16.

[20] Brown LA, Baker A. Shuttles and cycles: transport of proteins into the peroxisome matrix (review). Mol Membr Biol 2008;25:363–375.

[21] Wolf J, Schliebs W, Erdmann R. Peroxisomes as dynamic organelles: peroxisomal matrix protein import. FEBS J 2010;277:3268-3278.

[22] Domin N, Wilson D, Brock M. Methylcitrate cycle activation during adaptation of *Fusarium solani* and *Fusarium verticillioides* to propionyl-CoA-generating carbon sources. Microbiol 2009; 155:3903-3912.

[23] Kang PJ, Ostermann J, Shilling J, Neupert W, Craig EA, Pfanner N. Requirement for hsp70 in the mitochondrial matrix for translocation and folding of precursor proteins. Nature 1990;348:137-143.

[24] Werner-Washburne M, Becker J, Kosic-Smithers J, Craig E. Yeast Hsp70 RNA levels vary in response to the physiological status of the cell. J Bacteriol 1989;171:2680-2688.

[25] Chang Q, Petrash JM. Disruption of aldo-keto reductase genes leads to elevated markers of oxidative stress and inositol auxotrophy in *Saccharomyces cerevisiae*. Biochim Biophys Acta 2008;1783:237-245.

[26] Labbé G, de Groot S, Rasmusson T, Milojevic G, Dmitrienko GI, Guillemette JG. Evaluation of four microbial class II fructose 1,6-bisphosphate aldolase enzymes for use as biocatalysts. Protein Expr Purif 2011;80:224-233.

[27] Chang Ch-Y, HsiehY-Ch, Wang TY, Chen Y-Ch, Wang YK, Chiang TW, Chen YJ, Chang Ch-H, Chen Ch-J, Wu TK. Crystal structure and mutational analysis of

aminoacylhistidine dipeptidase from *Vibrio alginolyticus* reveal a new architecture of M20 metallopeptidases.J Biol Chem 2010;285:39500–39510.

[28] Thelen JJ, Muszynski MG, David NR, Luethy MH, Elthon TE, Miernyk JA, Randall DD. The dihydrolipoamide S-acetyltransferase subunit of the mitochondrial pyruvate dehydrogenase complex from maize contains a single lipoyl domain. J Biol Chem 1999;274:21769-21775.

[29] Nango E, Yamamoto T, Kumasaka T, Eguchi T. Structure of *Thermus thermophilus* homoisocitrate dehydrogenase in complex with a designed inhibitor. J Biochem 2011,150;607-614.

[30] Amata O, Marino T, Nino Russo N, Toscano M. A proposal for mitochondrial processing peptidase catalytic mechanism. J Am Chem Soc 2011;133:17824–17831.

[31] Takeda M, Katayam H, Satoh T, Mabuchi T. Three copies of the *ATP2* gene are arranged in tandem on chromosome X in the yeast *Saccharomyces cerevisiae*. Curr Genet 2005;47:265-272.

[32] Lapaille M, Thirty M, Perez E, González-Halphen D, Remacle C, Cardol P. Loss of mitochondrial ATP synthase subunit beta (Atp2) alters mitochondrial and chloroplastic function and morphology in Chlamydomonas. Biochim Biophys Acta, 2010;1797:1533-1539.

[33] Flores-Carreón A, Gómez-Villanueva A, San Blas G. Beta-1-3-glucanase and dimorphism in *Paracoccidioides brasiliensis*. Antonie Van Leeuwenhoek 1979;45:265-274.

[34] Kotani H, Kmiec EB, Holloman WK. Purification and properties of a cruciform DNA binding protein from *Ustilago maydis*. Chromosoma 1993;102:348-354.

[35] Dutta, S, Gerhold DL, Rice M, Germann M, Kmiec EB. The cloning and overexpression of a cruciform binding protein from *Ustilago maydis*. Biochim Biophys Acta 1997;1352:258-266.

[36] Skau CT, Kovar DR. Fimbrin and tropomyosin competition regulates endocytosis and cytokinesis kinetics in fission yeast. Curr Biol 2010;20:1415-1422.

ACCEPTED MANUSCRIPT

ACCEPTED MANUSCRIPT

[37] Goncalves RP, Buzhynskyy N, Prima V, Sturgis JN, Scheuring S. Supramolecular assembly of VDAC in native mitochondrial outer membranes. J Mol Biol 2007;369:413-418.

[48] Yehezkel G, Abu-Hamad S, Shoshan-Barmatz V. An N-terminal nucleotide-binding site in VDAC1: involvement in regulating mitochondrial function. J Cell Physiol 2007; 221:551-561

[39] Ross SJ, Findlay VJ, Malakasi P, Morgan BA, Thioredoxin peroxidase is required for the transcriptional response to oxidative stress in budding yeast. Mol Biol Cell 2000;11:2631-2642.

[40] Zelenaya-Troitskaya O, Perlman PS, Butow RA. An enzyme in yeast mitochondria that catalyzes a step in branched-chain amino acid biosynthesis also functions in mitochondrial DNA stability. EMBO J 1995;14:3268–3278.

[41] Kucej M, Kucejova B, Subramanian R, Chen XJ, Butow RA. Mitochondrial nucleoids undergo remodeling in response to metabolic cues. J Cell Sci 2008;121:1861-1869.

[42] Iacovino M, Granycome C, Sembongi H, Bokor-Brown M, Butow RA, Holt IJ, Bateman JM. The conserved translocase Tim 17 prevents mitochondrial DNA loss. Hum Mol Genet 2009;18:65-74.

[43] Nishi T, Forgac M. The vacuolar (H1)-ATPases: nature's most versatile proton pumps. Nat Rev Mol Cell Biol 2002;3:94-103.

[44] Vos WL, Vermeer LS, Hemminga MA. Conformatin of a peptide encompassing the proton transolocation cannel of vacuolar H^+-ATPase. Biophys J 2007;92:138-146.

[45] Tang Y, Sieg A, Trotter PJ. ^{13}C-metabolic enrichment of glutamate in glutamate dehydrogenase mutants of *Saccharomyces cerevisiae*. Microbiol Res 2011;166:521-530.

[46] Yogev O, Yogev O, Signer E, Shaulian E, Godlberg M, Fox TD, Pines O. Fumarase: a mitochondrial metabolic enzyme and a cytosolic/nuclear component of the DNA damage response. Plos Biology 2010; PLoS Biol 8:e1000328.

[47] John GB, Shang Y, Renken C, Mannella CA, Selker JML, Rangell L, Bennett MJ, Zha J. The mitochondrial inner membrane protein mitofilin controls cristae morphology. Mol Biol Cell 2005;16:1543-1554.

ACCEPTED MANUSCRIPT

[48] Frerman FE. Acyl-CoA dehydrogenases, electron transfer flavoprotein and electron transfer flavoprotein dehydrogenase. Biochem Soc Trans 1988;16:416–418.

[49] Filling C, Berndt KD, Benach J, Knapp S, Prozorovski T, Nordling E, Ladenstein R, Jörnvall H, Oppermann U. Critical residues for structure and catalysis in short-chain dehydrogenases/reductases. J Biol Chem 2002;277:25677-25684.

[50] Kallberg Y, Oppermann U, Jörnvall H, Persson B. Short-chain dehydrogenases/reductases (SDR): coenzyme-based functional assignments in completed genomes. Eur J Biochem 2002;269:4409–4417.

[51] Wei H, Requena N, Fisher R. The MAPKK kinase SteC regulates conidiophore morphology and is essential for heterokaryon formation and sexual development in the homothallic fungus *Aspergillus nidulans*. Mol Microbiol 2003;47:1577-1588.

[52] Gonzalez Y, Meerbrey K, Chong J, Toril Y, Padte NN, Sazer S. Nuclear shape, growth and integrity in the closed mitosis of fission yeast depende on the Ran-GTPase system, the spindle pole body and the endoplasmic reticulum. J Cell Sci 2009;122:2464-2472.

[53] Medendorp K, van Groningen JJM, Vreede L, Hetterschijt L, van de Hurk WH, de Bruijn RH, Brugmans L, van Kessel AG. The mitotic arrest deficient protein MAD2B interacts with the small GTPase RAN throughout the cell cycle. PlosOne 2009;4:e7020.

[54] Graña X, Pérez de la Ossa P, Broceño C, Stöcker M, Gariga J, Puigdoménech P, Climent F. 2,3-bisphospoglycerate-independent phosphoglycerate mutase is conserved among different phylogenic kingdoms. Comp Biochem Physiol B Biochem Mol Biol 1995;112:287-293.

[55] Grein S, Pyerin W. BTF3 is a potential new substrate of protein kinase CK2. Mol Cell Biochem 1999;191:121-128.

[56] Welch AK, Bostwick CJ, Cain BD. Manipulations in the peripheral stalk of the *Saccharomyces cerevisiae* F1F0-ATP synthase. J Biol Chem 2011;286:10155-10162.

[57] Homiquist, M. Alpha/Beta-Hydrolase fold enzymes: structures, functions and mechanisms. Curr Protein Pept Sci 2000;1:209-235.

ACCEPTED MANUSCRIPT

[58] Ziólkowska NE, Karotki L, Rehman M, Huiskonen JT, Walther TC. Eisosome-driven plasma membrane organization is mediated by BAR domains. Nat Struct Mol Biol 2011;18:854-856.

[59] Atir-Lande A, Gildor T, Kornitzer D. Role for the SCFCDC4 ubiquitin ligase in *Candida albicans* morphogenesis. Mol Biol Cell 2005;16:2772-2785.

[60] Takeda Y, Noguchi T. Characteristics of alanine: glyoxylate aminotransferase from *Saccharomyces cerevisiae*, a regulatory enzyme in the glyoxylate pathway of glycine and serine biosynthesis from tricarboxylic acid-cycle intermediates. Biochem J 1985;231:157-163.

[61] Flom G, Weekes J, Williams JJ, Johnson JL. Effect of mutation of the tetratricopeptide repeat and asparatate-proline 2 domains of Sti1 on Hsp90 signaling and interaction in *Saccharomyces serevisiae*. Genetics 2006;172:41-51.

[62] Ferreira-Cerca S, Poll G, Gleizes PE, Tschochner H, Milkereit P. Roles of eukaryotic ribosomal proteins in maturation and transport of pre-18S rRNA and ribosome function. Mol Cell 2005;20:263–275.

[63] Orrú S, Aspesi A, Armiraglio M, Caterinos M, Loreni F, Ruoppolo M, Santoro C, Dianzani I. Analysis of the ribosomal protein S19 interactome. Mol Cell Proteomics 2007;6.3:382-393.

[64] Pareek G, Samaddar M, D´Silva P. Primary sequence that determines the functional overlap between mitochondrial heath shock protein 70 Ssc1 and Ssc3 of *Saccharomyces cerevisiae*. J Biol Chem 2011;286:19001-19013.

[65] Westermann B, Prip-Buus C, Neupert W, Schwarz E. The role of the GrpE homologue, Mge1p, in mediating protein import and protein folding in mitochondria. EMBO J 1995;14:3452-3460.

[66] Kim SY, Kim, J. Roles of dihydrolipoamide dehydrogenase Lpd1 in *Candida albicans* filamentation. Fungal Genet Biol 2010;47:782–788.

ACCEPTED MANUSCRIPT

Figure Legends

Fig. 1. Morphology of *U. maydis* FB2*wt,* constitutive yeast (CL211), and constitutive mycelial (GP25) cells. Upper three panels: cells grown in synthetic medium at pH 7. Lower three panels: cells growing in synthetic medium at pH 3. Cells were stained with cotton blue and observed in a bright field optics microscopy.

Fig. 2. Coomassie-stained 2-DE gels of total soluble proteins extracts from *U. maydis* and zoomed images of representative spots. Proteins were extracted from wild type FB2*wt* cells and from CL211 and GP25 constitutive yeast and mycelia mutants, respectively. All cells were grown at pH 7 and pH 3. Upper part, proteins were separated by IEF using nonlinear pH 5-8 strips followed by 12% SDS-PAGE separation. Differentially accumulated proteins are numbered and referenced in Table 1 and Supplementary Table 1. Lower part, showed zoomed images of some representative spots when comparing the three strains when were grown either at pH 7 or pH 3. UM03285=CipC; UM00496=Hmp; UM00961=H^+ATPase; UM03006=aldo-keto-reductase.

Fig. 3. Identification of *U. maydis* differentially accumulated proteins in response to change in the pH of growth media. The three strains used were grown at pH 7 or pH 3 and their 2-DE protein profiles were analyzed as described in Materials and Methods section. The differentially expressed proteins at pH 7 or pH3 in each of the strains were identified, and the data were used to construct the Venn diagrams. A) Up-accumulated proteins at pH 3; B) Down-accumulated proteins at pH 3. The intersections represent the proteins that are shared among all strains. Relative morphology observed at pH 7 or pH 3, respectively is represented by small sketches.

ACCEPTED MANUSCRIPT

Fig. 4. Identification of *U. maydis* differentially accumulated proteins in response to dimorphism. The three strains used were grown at pH7 or pH 3, their 2-DE protein profiles were analyzed as described in Materials and Methods section. The following comparison were made: **a**: FB2*wt* at pH 3 (mycelium) *vs* FB2*wt* at pH 7 (yeast); **b**: FB2*wt* at pH 7 (yeast) *vs* GP25 at pH 7 (mycelium), and **c**: FB2*wt* at pH 3 (mycelium) *vs* CL211 at pH 3 (yeast). The three comparisons have in common a change in morphology. The data were used to construct Venn diagrams. A) Up-accumulated proteins in the mycelial form. B) Down-accumulated proteins in the mycelial form. The intersections represent the proteins that are shared among strains and related to dimorphism. Relative morphology observed at each comparison is represented by small sketches.

ACCEPTED MANUSCRIPT

ACCEPTED MANUSCRIPT

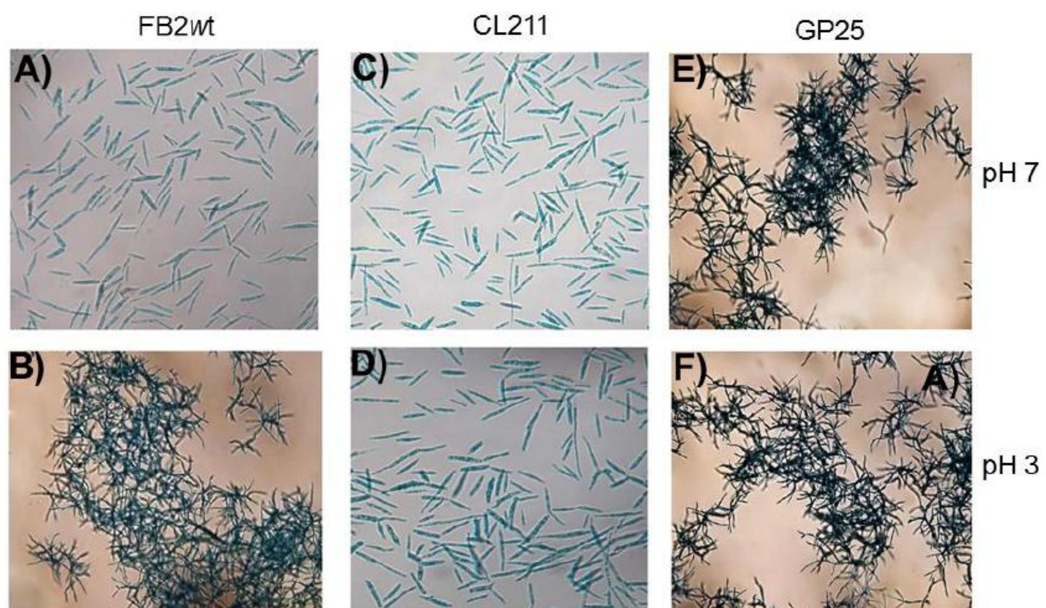

Fig. 1

ACCEPTED

ACCEPTED MANUSCRIPT

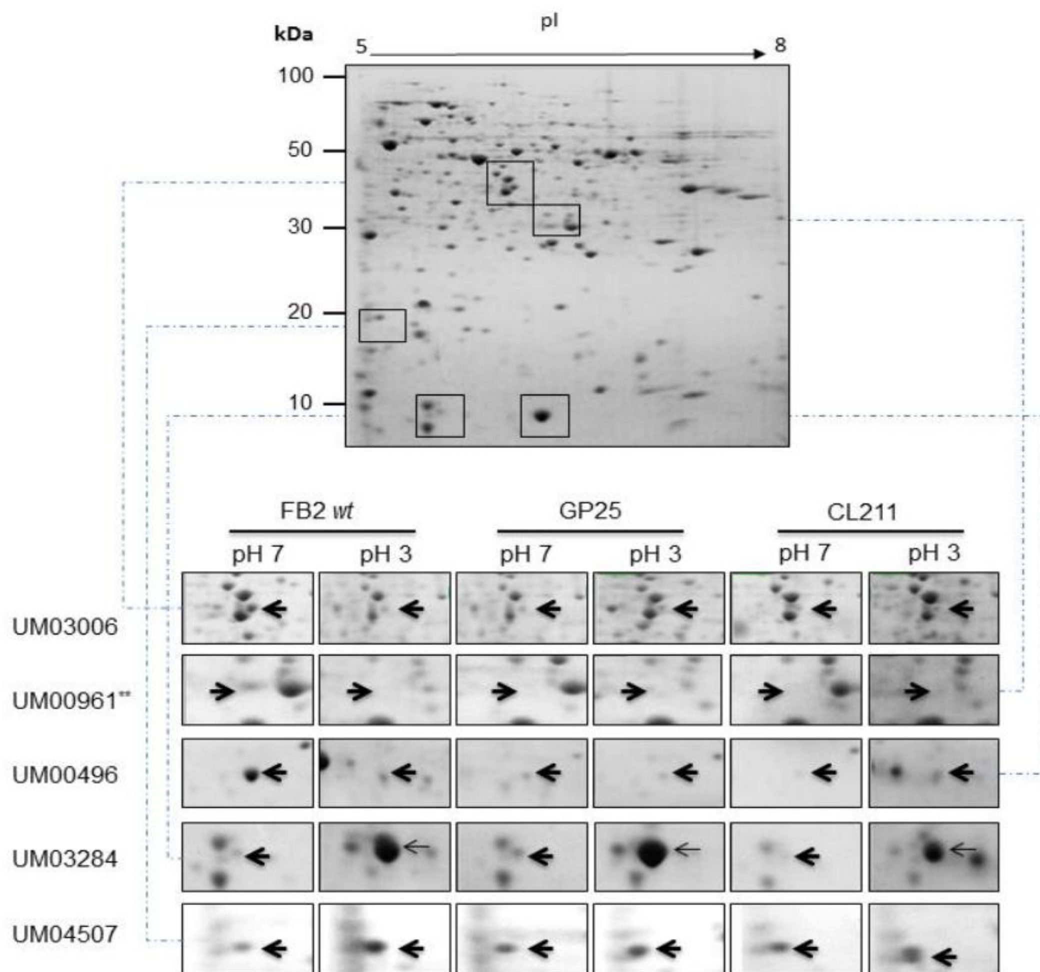

Fig. 2

ACCEPTED MANUSCRIPT

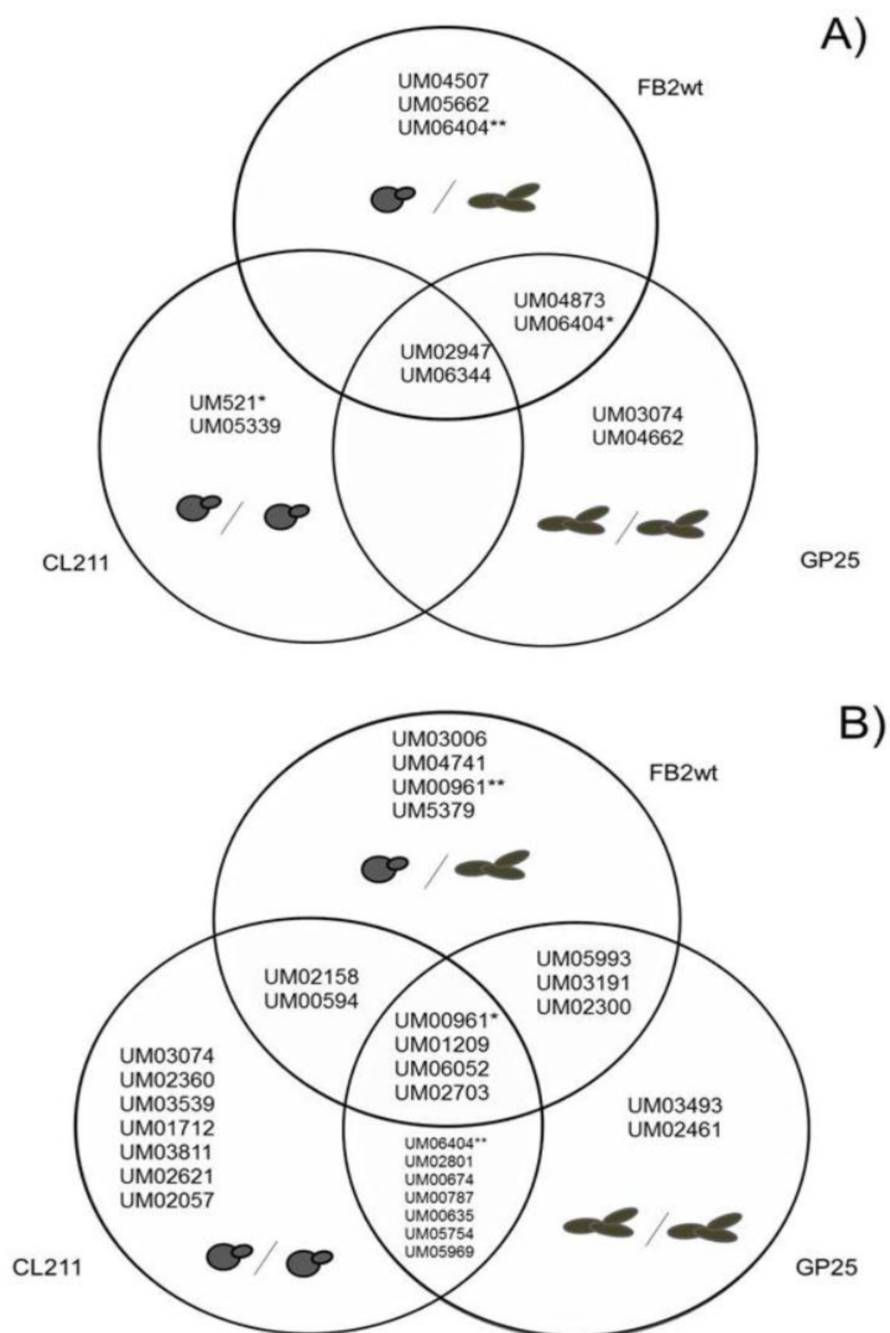

Fig. 3

ACCEPTED MANUSCRIPT

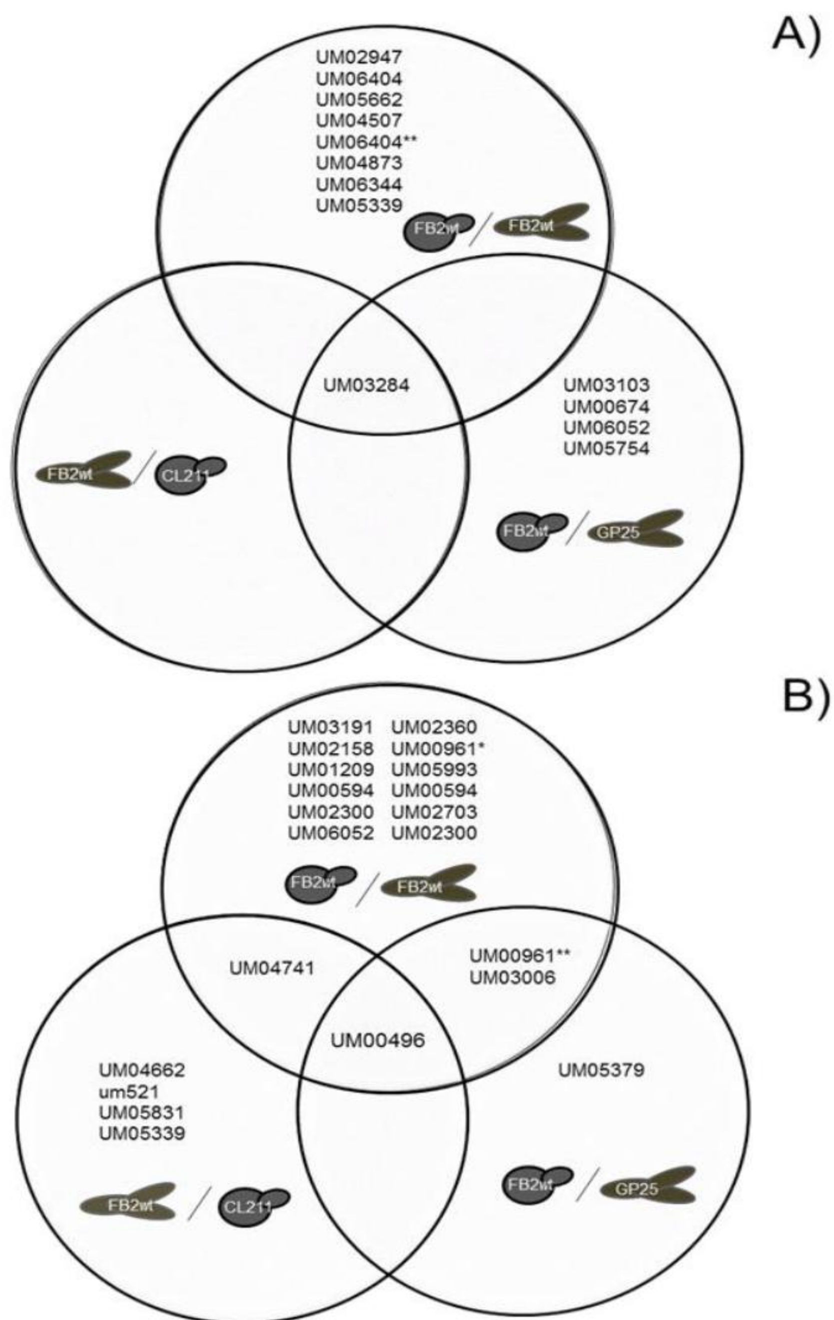

Fig. 4

ACCEPTED MANUSCRIPT

Table 1. Protein spots up- and down-accumulated after transition of FB2wt from budding-yeast to filament induced by pH changes

Spot	MUMDB Accession No	Description	%vol		Ratio	MW/pI Exptl.	MW/pI Theo.
			pH 7	pH 3			
Up-accumulated							
20	UM02947	peroxisomal membrane protein (um10331)	0.7179	1.6569	2.31	21.0/6.45	18.3/6.11
35	UM06404*	thioredoxin peroxidase	0.2067	0.3935	1.90	27.0/6.35	24.6/5.98
54	UM05662	mitochondrial porin	0.2952	0.6644	2.25	21.0/8.0	31.9/9.97
19	UM04507	TPM2-tropomyosin isoform 2 (um11985)	0.0567	3.3833	5.95	20.0/5.15	18.6/4.79
125	UM03284	conserved hypothetical protein (CipC)	0.3341	4.6902	14.04	12.0/5.5	12.1/5.33
42	UM06404**	thioredoxin peroxidase	0.838861	1.49819	1.79	28.0/6.35	24.6/5.98
89	UM04873	probable LYS12 - Homo-isocitrate dehydrogenase	0.19271	0.33502	1.74	45.0/6.83	40.7/6.78
113	UM06344	2-methylcitrate dehydratase	0.110988	0.20139	1.81	58/6.8	60.2/8.35
Down-accumulated							
1	UM00496	cruciform DNA recognition protein Hmp1 (umd11-30)	1.6732	0.3079	5.43	10.5/6.25	10.1/7.53
70	UM03006	aldo-keto reductase yakc [NADP+]	0.4291	0.2181	1.97	38.0/6.1	37.9/5.84
80	UM04741	ILV5-ketol-acid reductoisomerase (mitochondrial) (um10681)	0.4254	0.176	2.42	42.0/5.97	44.7/8.12
108	UM03191	ATP2 - F1F0-ATPase complex, F1 beta subunit (um10397)	2.0965	1.0509	1.99	50.0/5.2	57.2/5.5
113	UM05379	H+-ATP synthase alpha chain, mitochondrial (um10213)	0.4898	0.1223	4.00	55.0/7.25	58.4/9.74
22	UM02360	conserved hypothetical protein	1.4422	0.4321	3.34	21.0/5.45	
48	UM00961*	conserved hypothetical protein	1.2558	0.217	5.79	30.0/6.5	31.6/6.6
50	UM00961**	conserved hypothetical protein	0.7536	0.1956	3.85	30.0/6.3	31.6/6.6
109	UM02158	conserved hypothetical protein	0.7285	0.2778	2.62	51.0/5.67	51.9/5.34
121	UM01209	SSC-mitochondrial HSP70 member	1.35509	0.505524	2.68	75.0/5.5	72.1/5.62
126	UM06052	oxidoreductase, aldo/keto reductase family (um11598)	0.251062	0	ND	33.0/6.45	33.1/6.09
127	UM06404***	thioredoxin peroxidase	0.420716	0.23486	1.79	27.0/6.05	24.6/5.98
128	UM02703	probable FBP1 - fructose-1,6-bisphosphatase	0.283052	0.0779723	3.63	43.0/5.63	37.8/5.09

ACCEPTED MANUSCRIPT

105	UM05993	probable MAS1 - mitochondrial processing peptidase beta chain precursor	0.331101	0.204501	1.62	50.0/5.97	52.6/6.39
130	UM00594	probable dihydrolipoamide acetyltransferase component of pyruvate dehydrogenase complex, mitochondrial precursor	0.418683	0.0791991	5.29	63.0/5.78	52.5/6.82
131	UM02300	probable alpha-amylase	0.309948	0.101145	3.06	67.0/5.63	60.8/5.36

ACCEPTED MANUSCRIPT

ACCEPTED MANUSCRIPT

Table 2. Protein spots up- and down-accumulated in constitutive mycelium GP25 mutant induced by pH changes

Spot	MUMDB Accession No.	Description	%vol		Ratio	MW/pI Exptl.	MW/pI Theo.
			pH 7	pH 3			
Up-accumulated							
53	UM06404**	thioredoxin peroxidase	0.8467	1.6327	1.93	27.5/6.35	24.6/5.98
7	UM03284	conserved hypothetical protein (CipC)	0.4285	5.4568	12.73	12/5.5	12.1/5.33
21	UM02947	peroxisomal membrane protein (um10331)	0.615383	1.03838	1.69	21.0/6.45	18.3/6.11
140	UM06344	2-methylcitrate dehydratase	0	0.214619	ND	58/6.8	60.2/8.35
141	UM03074	probable transcription factor BTF3a	0	0.567454	ND	20.5/5.7	17.7/5.16
142	UM04873	probable LYS12 - Homo-isocitrate dehydrogenase	0.182231	0.352763	1.94	45.0/6.83	40.7/6.78
1	UM04662	RPS19B-ribosomal protein S19 (um11551)	0.1682	0.4469	2.66	18.0/5.9	17.7/5.07
Down-accumulated							
34	UM03493	MGE1-heat shock protein - chaperone	0.3788	0.1999	1.90	24.0/5.67	27.4/9.85
133	UM01209	SSC-mitochondrial HSP70 member	3.4175	1.4591	2.34	74.0/5.5	72.1/5.62
69	UM06052	oxidoreductase, aldo/keto reductase family (um11598)	0.5291	0.2202	2.40	32.0/6.5	33.1/6.09
90	UM00674	FBA-fructose-bisphosphate aldolase	1.4567	0.6992	2.08	38.0/6	39.3/5.5
116	UM02801	NADP-specific glutamate dehydrogenase	1.0499	0.2184	4.81	48.0/6.8	49.6/6.64
118	UM00787	FUM-fumarate hydratase (um10787)	0.8139	0.3407	2.39	48.5/6.95	54.8/8.21
131	UM00635	conserved hypothetical protein	0.3924	0.1145	3.43	75.0/6.5	74.1/6.95
124	UM03191	probable ATP2 - F1F0-ATPase complex, F1 beta subunit (um10397)	2.13969	1.25185	1.71	50.0/5.2	57.2/5.5
143	UM00961*	conserved hypothetical protein	1.09131	0.263302	4.14	30.0/6.5	31.6/6.6
70	UM05969	related to short-chain alcohol dehydrogenase (um10898)	0.344472	0.220098	1.57	32.0/6.35	30.6/6.17
77	UM05754	probable electron transfer flavoprotein alpha chain precursor	0.630345	0.323788	1.95	34.0/5.3	36.5/5.36
47	UM06404***	thioredoxin peroxidase	0.340138	0.208478	1.63	27.0/6.05	24.6/5.98

37

ACCEPTED MANUSCRIPT

102	UM02703	probable FBP1 - fructose-1,6-bisphosphatase	0.225422	0.0970464	2.32	43.0/5.63	37.8/5.09
122	UM05993	probable MAS1 - mitochondrial processing peptidase beta chain precursor	0.379085	0.192763	1.97	50.0/5.97	52.6/6.39
123	UM02461	probable LPD1 - dihydrolipoamide dehydrogenase precursor	0.529943	0.284174	1.86	50.0/5.97	53.6/7.55
144	UM02300	probable alpha-amylase	0.147111	0.0732693	2.01	67.0/5.63	60.8/5.36

ACCEPTED MANUSCRIPT

ACCEPTED MANUSCRIPT

Table 3. Protein spots up- and down-accumulated in constitutive yeast CL211 mutant induced by pH changes

Spot	MUMDB Accession No.	Description	%vol		Ratio	MW/p*I* Exptl.	MW/p*I* Theo.
			pH 7	pH 3			
Up-regulated							
47	um521*	GTP-binding nuclear protein RAN [*Ustilago maydis* 521]	0.4903	0.906857	1.85	25.0/6.95	24.5/6.6
49	UM05339	2,3-bisphosphoglycerate-dependent phosphoglycerate mutase	0.2597	0.861759	3.32	26/6.7	22.9/6.38
112	UM06344	2-methylcitrate dehydratase	0.1268	0.312818	2.47	58/6.8	60.2/8.35
34	UM02947	peroxisomal membrane protein (um10331)	0.6489	1.28025	1.97	21/6.45	18.3/6.11
Down-regulated							
33	UM03074	transcription factor BTF3a	1.0624	0.4155	2.56	20.5/5.7	17.7/5.16
121	UM01209	SSC1-mitochondrial HSP70 member	1.7771	0.692	2.64	74.0/5.5	72.1/5.62
67	UM05969	short-chain alcohol dehydrogenase (um10898)	0.4574	0.1969	2.32	32.0/6.35	30.6/6.17
70	UM05754	electron transfer flavoprotein alpha chain precursor	0.4519	0.2165	2.09	34.0/5.3	36.5/5.36
103	UM00787	FUM1-fumarate hydratase (um10787)	1.3086	0.5891	2.22	48.5/6.95	54.8/8.21
35	UM02360	conserved hypothetical protein	1.3439	0.4948	2.72	21.0/5.45	13.8/6.53
69	UM03539	conserved hypothetical protein	0.6608	0.2999	2.20	34.0/5.92	36.1/5.78
109	UM02158	conserved hypothetical protein	0.7926	0.3933	2.02	50.0/5.2	51.9/5.34
61	UM00961*	conserved hypothetical protein	0.816201	0.194338	4.20	30.0/6.5	31.6/6.6
66	UM06052	related to oxidoreductase, aldo/keto reductase family (um11598)	0.633697	0.366476	1.73	33.0/6.45	33.1/6.09
79	UM00674	probable FBA1 - fructose-bisphosphate aldolase	1.23014	0.663349	1.85	38.0/6	39.3/5.5
101	UM02801	probable NADP-specific glutamate dehydrogenase	2.47029	1.21665	2.03	48.0/6.8	49.6/6.64
118	UM00635	conserved hypothetical protein	0.465587	0.288195	1.62	75.0/6.5	74.1/6.95
53	UM06404***	thioredoxin peroxidase	0.472615	0.223473	2.11	27.0/6.05	24.6/5.98
63	UM01712	conserved hypothetical protein	0.590076	0.185385	3.18	31.0/6.72	27/6.79
65	UM03811	probable SOL1 - Protein with a possible role in tRNA export	0.302811	0.152138	1.99	32.0/5.67	30.3/5.15

ACCEPTED MANUSCRIPT

85	UM02703	probable FBP1 - fructose-1,6-bisphosphatase	0.282049	0.138097	2.04	43.0/5.63	37.8/5.09
88	UM02621	probable AGX1 - alanine-glyoxylate transaminase	0.481356	0.192486	2.50	44.0/6.57	42/6.52
127	UM00594	probable dihydrolipoamide acetyltransferase component of pyruvate dehydrogenase complex, mitochondrial precursor	0.344815	0.198942	1.73	63.0/5.78	52.5/6.82
119	UM02057	probable STI1 - Hsp90 cochaperone	0.287264	0.135092	2.13	76.0/5.93	66.3/5.43

ACCEPTED MANUSCRIPT

40

ACCEPTED MANUSCRIPT

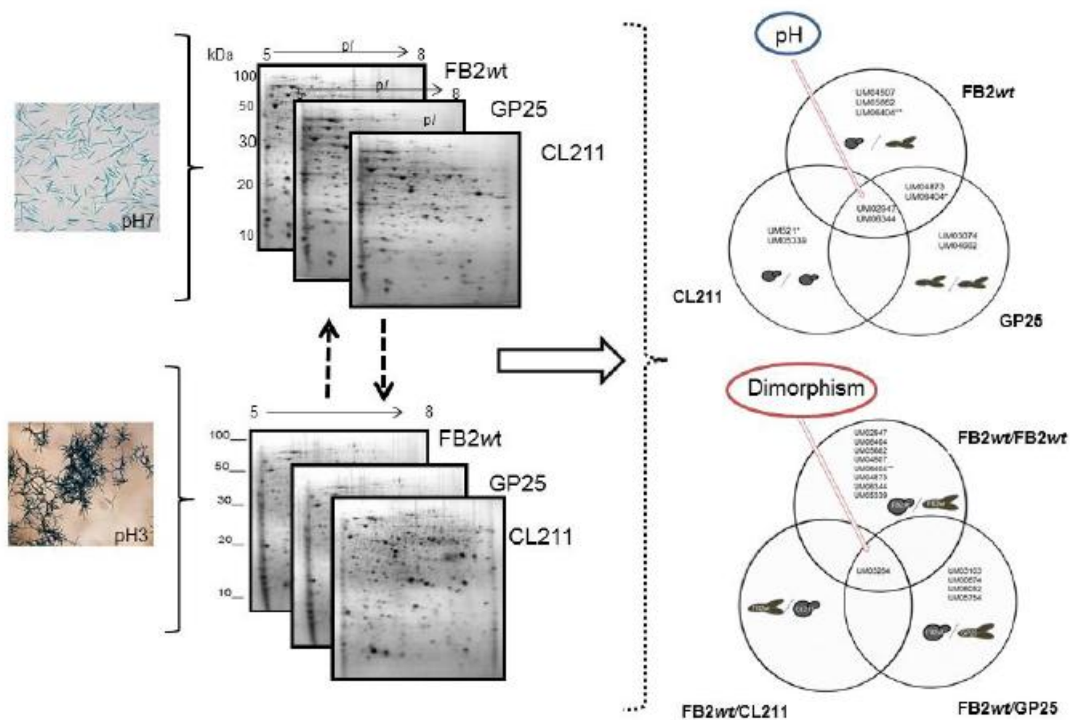

Graphical abstract

ACCE

ACCEPTED MANUSCRIPT

Highlights

1. *Ustilago maydis* proteome map was most representative in the range of pH from 5-8.
2. *Ustilago maydis* can form filaments *in vitro* in response to acidic pH
3. Constitutive yeast and mycelia mutants (CL211 and GP25, respectively)
4. Dimorphic related proteins and mutants related proteins were detected

ACCEPTED MANUSCRIPT

Supplementary information

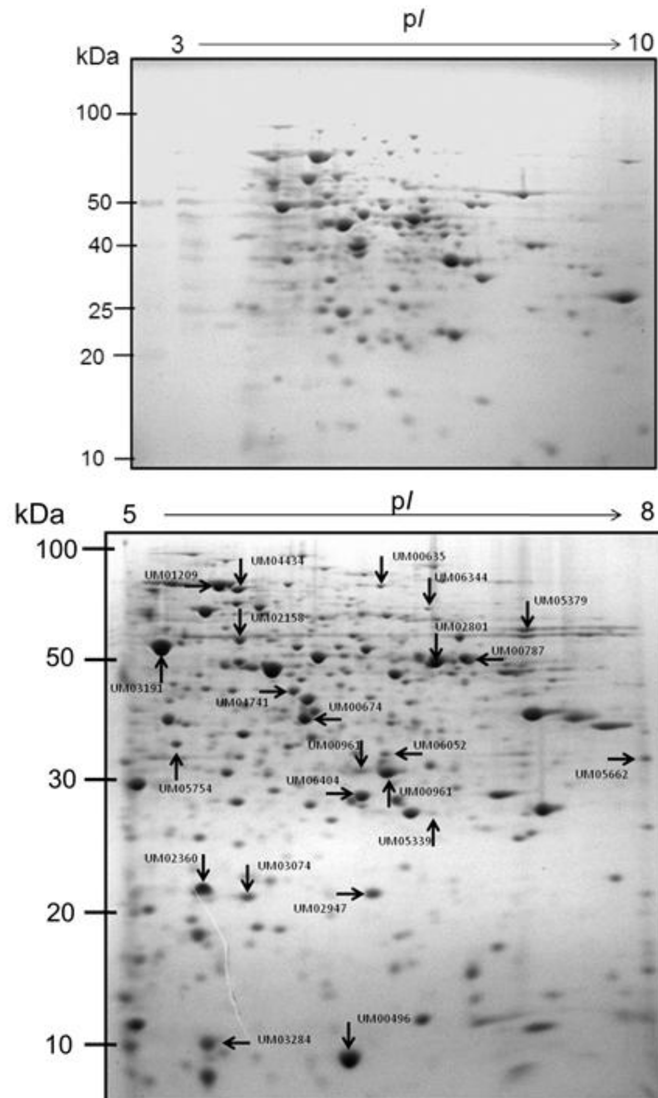

Fig. S1. 2-DE protein profile of total soluble proteins obtained from *U. maydis* wild type strain (FB2*wt*). Proteins were extracted using the acidic extraction protocol as described in materials and methods section. Gels were stained with Coomassie colloidal blue. A) 2DE patterns in the range of pH 3-10, B) in the range of pH 5-8. Arrows indicates some differential proteins as shown in Fig. 3.

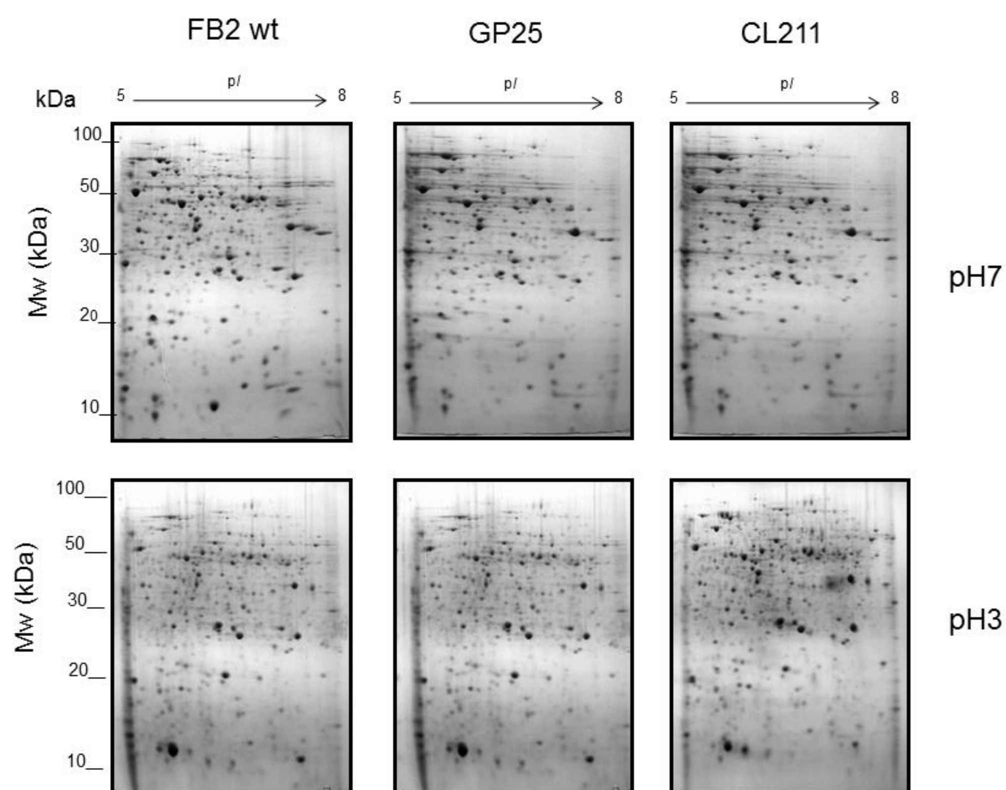

Fig. S2. 2-DE patterns of proteins extracted from wild type FB2*wt* cells, GP25, and CL211 cells, constitutive mycelia and yeast mutants. Cells were grown in synthetic media at pH7 (upper-panel) or pH 3 (lower-panel). Proteins were separated by IEF using nonlinear strips in the range of pH 5-8 followed by second dimension separation in 12% SDS-PAGE gels. Gels were stained with Coomassie colloidal blue.

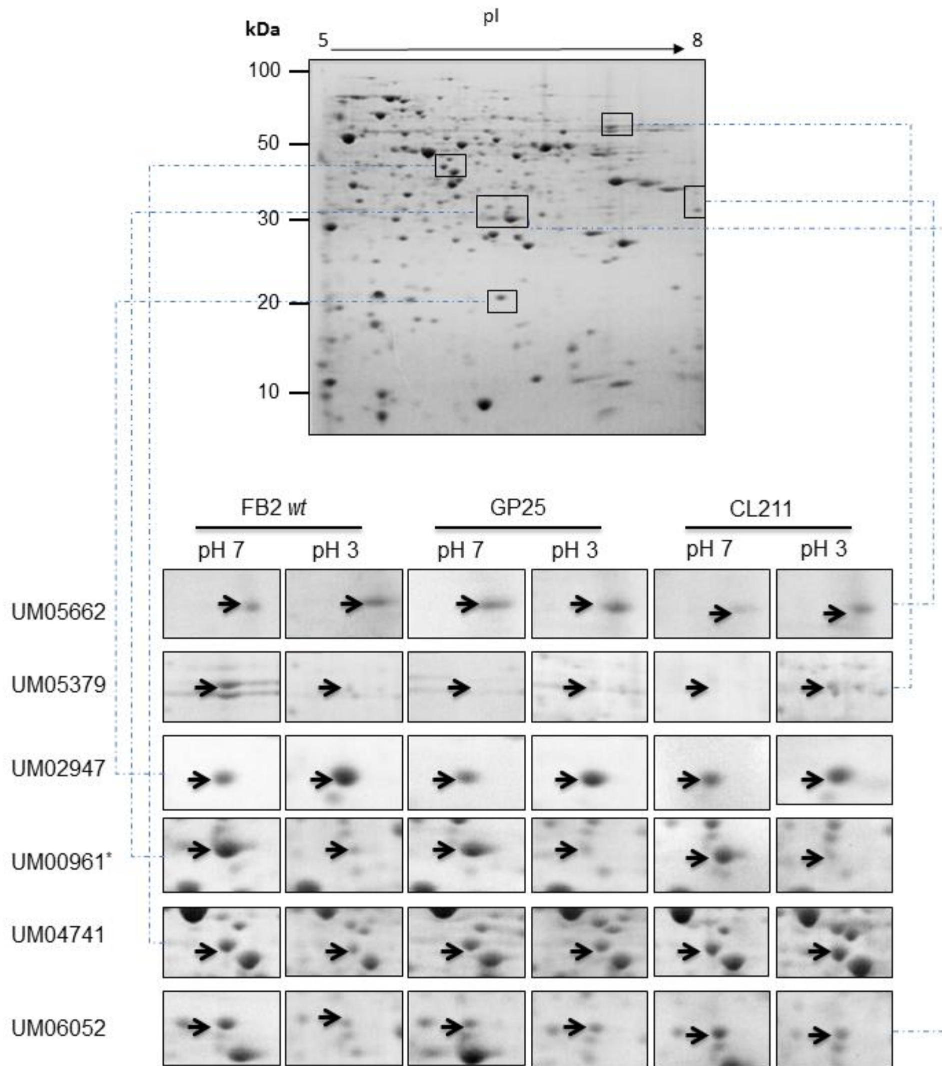

Fig. S3. Coomassie-stained 2-DE gels of total soluble proteins extracts from *U. maydis*. Proteins were extracted from wild type FB2*wt* cells and from CL211 and GP25 constitutive mycelia and yeast cells, respectively. All cells were grown in synthetic media at pH 7 and pH 3. Proteins were separated by IEF using nonlinear pH 5-5 strips followed by 12% SDS-PAGE. All spots with protein identifications are numbered and are referenced in Table 1 and Supplementary Table 1. Zoomed images of some representative spots when comparing FB2*wt* with constitutive mycelia mutant GP25, or yeast constitutive mutant CL211 grown at pH 7 or 3. UM05662=mitochondrial porin; UM05379= H+-ATP synthase alpha chain, mitochondrial (um10213); UM2947=peroxisomal membrane protein; UM00961*=conserved hypothetical protein; UM04741=ILV5-ketol-acid reducoisomerase; UM06052=oxidoreductase.

VI. CONCLUSIONES

En el presente trabajo se mejoró la resolución de las manchas proteicas en el análisis de geles bidimensionales, mediante el método de extracción en condiciones ácidas, para el análisis de proteínas diferencialmente acumuladas en tres cepas de *Ustilago maydis* FB2*wt*, CL211 levadura constitutiva y GP25 micelio constitutiva, cuando son sometidas al cambio de pH de 7 a 3 el cual induce la transición de levadura a micelio en la cepa silvestre.

La resolución de los geles permitió la separación de 404 manchas proteicas, de las cuales fue posible la identificación de 43 proteínas. Mediante el empleo de diagramas de Venn se clasificaron en aquellas relacionadas con el dimorfismo inducido por el cambio de pH, proteínas que son afectadas por el pH y proteínas cuya acumulación es afectada por la mutación en la via MAPK (CL211) o en la desacetilasa de histonas (GP25). Mediante este análisis se contribuye con la generación de información de proteínas que son diferencialmente reguladas por los efectos anteriormente dichos en el hongo modelo *Ustilago maydis*.

VII. REFERENCIAS

Aebersold R. and Mann M. 2003. Quantitative proteome analysis: methods and applications. Nature 422, 198-207.

Aréchiga-Carvajal E.T., Ruiz-Herrera J. 2004. The *RIM101/pacC* homologue from the Basidiomycete *Ustilago maydis* is functional in multiple pH-sensitive phenomena. Eukaryot. Cell. 4, 999-1008.

Bölker M. 2001. *Ustilago maydis* a valuable model system for the study of fungal dimorphism and virulence. Microbiology. 147. 1395-1401

Bonifaz A. 2000. Micología Médica Básica 2a edicion, Mendez editores. "*Introducción a la micología*" p. 4.

Böhmer M., Colby T., Böhomer C., Bräutigam A. and Bölker M. 2007. Proteomic analysis of dimorphic transition in the phytopathogen fungus *Ustilago maydis.* Proteomics. 7. 675-685.

Brefort T., Doehlemann G., Mendoza-Mendoza A., Reissmann S., Djamei A and Kahmann R. 2009. *Ustilago maydis* as pathogen. Annu Rev. Phytopathol. 47:423-445.

Cabezón V. 2009. Respuesta de Candida albincans tras su interacción con el macrófago: análisis proteómico y estudio de marcadores de apoptosis. Tesis doctoral Universidad Complutense de Madrid. p. 54-56.

Cabrera-Ponce J.L., León-Ramírez C., Verver-Vargas A., Palma-Tirado L. and Ruiz-Herrera J. 2012. Metamorphosis of the Basidiomycota *Ustilago maydis*: Transformation of yeast-like cells into basidiocarps. Fungal Genetics Biology (2012), http://dx.doi.org/10.1016/j.fgb.2012.07.005

Davis D. 2003. Adaptation to enviromental pH in *Candia albicans* and its relation to pathogenesis. Curr Genet. 44, 1-7.

Deacon Jim. 2006. Fungal Biology 4th ed. "Diferentiation and development" p.85-86

Djamei Armin and Kahmann Regine. 2012. *Ustilago maydis*: dissecting the molecular interface between pathogen and plant. PLOS Pathogens. 8 (11) e1002955.doi: 10.1371/journal.ppat.1002955.

Feldbrüge M., Kämper J., Steinberg G. and Kahmann R. 2004. Regulation of mating and pathogenic development in *Ustilago maydis*. Current Opinion in Microbiology. 7, 666-672.

González-Fernández R., Prats E. and Jorrín-Novo J.V. 2009. Proteomics of plants pathogenic fungi. Journal of Biomedicine and Biotechnology. Volume 2010, Article ID 932527, 36 pages. doi:10.1155/2010/932527

Graves P.R. and Haystead T.A.J. 2002. Molecular Biologist´s Guide to Proteomics, Microbiology and Molecular Biology Reviews, Vol. 66 No. 1, 39-63.

Herrera Teófilo y Ulloa Miguel. 1998. El reino de los hongos, micología básica y aplicada "*Hongos verdaderos*" p. 294-295.

Kaffarnik F., Müller P., Leibundgut M., Kahmann R. And Feldbrügge M. 2003. PKA and MAPK phosphorylation of Prf1 allowz promoter discrimination in *Ustilago maydis*. The EMBO Journal. 22: 5817-5826.

Kämper J., Reichmann M., Romeis T., Bölker M., Kahmann R. 1995. Multiallelic recognition: nonself-dependent dimerization of the bR and bW homeodomain proteins in *Ustilago maydis*. Cell. 81 73-83.

Kamper J., Kahmann R., Bolker M., Ma L.J., Brefort T., Saville B., Banuett F., Kronstad J. W., Gold S., Muller O., Perlin, Wosten H., Vries R., Ruiz-Herrera J., Reynaga-Peña C., Snetselaar K., McCann M, Perez-Martın J., Feldbrügge M., Basse C., Steinberg G., Ibeas J., Holloman W., Guzman P., Farman M., Stajich J., Sentandreu R., Gonzalez-Prieto J., Schirawski J., Mendoza-Mendoza A., Greilinger D., Munch K., Rossel N., Kennell J., Molina L., Scherer M., Vranes M., Ladendorf O., Vincon V., Fuchs U., Sandrock B., Meng S., Ho E., Cahill M.J., Boyce K., Klose J., Klosterman S.J., Deelstra H., Ortiz-Castellanos L., Li W., Sanchez-Alonso P., Schreier P., Hauser-Hahn I., Vaupel M., Koopmann E., Friedrich G., Voss H., Schluter T., Margolis J., Platt D., Swimmer C., Gnirke A., Chen F., Vysotskaia V., Mannhaupt G., Guldener U., Munsterkotter M., Haase D., Oesterheld M., Mewes H.W., Mauceli E., DeCaprio D., Wade C., Butler J., Young S., Jaffe D., Calvo S., Nusbaum C., Galagan J. & Birren B. 2006. Insights from the genome of biotrophic fungal plant pathogen *Ustilago maydis*. Nature. 444: 97-101.

Lee K.H. 2001. Proteomics a technology-driven and technology-limited discovery science.Trends Biotechnol. 19, 217-222.

Mahlert M., Leveleki L., Hlubek A., Sandrock B., Bölker M. 2006. Rac1 and Cdc42 regulate hyphal growth and cytokinesis in the dimorphic fungus *Ustilago maydis*. Molecular Microbiology. 59, 567-578.

Martínez-Espinoza A., Leon C., Elizarraraz G. and Ruiz-Herrera J. 1997. Monomorphic nonpathogenic mutants of *Ustilago maydis*. Phytopathology 87:259-265

Martínez-Espinoza A., Garcia-Pedrajas M. and Gold S. 2002. The Ustilaginales as plant pest and model system. Fungal Genetics and Biology. 35, 1-20.

Martínez-Espinoza A., Ruiz-Herrera J. Leon-Ramírez C. and Gold S. 2004. MAP kinase and cAMP signaling pathways modulate the pH induced yeast to mycelium dimorphic transition in the corn smut fungus *Ustilago maydis*. Current Microbiology. 49. 274-281.

Monteoliva L., Martínez R., Pitarch A., Hernández M.L., Serna A., Nombela C., Albar J.P., Gil C. 2011.Quantitative proteome and acidic subproteome profiling of *Candida albicans* yeast to hypha transition. Journal of proteome research. 10, 502-217.

Morales-Vargas A.T., Dominguez A. and Ruiz-Herrera J. 2012. Identification of dimorphism-involved genes of *Yarrowia lipolytica* by means of microarray analysis, Research in Microbiology (2012), doi:10.1016/j.resmic.2012.03.002.

Morrow C. A. and Fraser J.A. 2009. Sexual reproduction and dimorphism in the pathogenic basidiomycetes. FEMS Yeast Res. 9(2): 161-177

Robledo-Briones M. and Ruiz-Herrera J. 2012. Regulation of genes involved in cell wall synthesis and structure during *Ustilago maydis* dimorphism. FEMS Yeast Research. DOI: 10.1111/1567-1364.12011.

Ruíz-Herrera J., León C., Guevara-Olvera L., Cárabez-Trejo A. 1995. Yeast-mycelial dimorphism of haploid and diploid strains of *Ustilago maydis*. Microbiol. 141, 695-703

Ruiz-Herrera J. and Martínez-Espinoza A.D. 1998. The fungus Ustilago maydis, from the aztec cuisine to research laboratory. Int. Microbiol. 1:148-158.

Sánchez-Martínez C. and Pérez-Martin J. 2001. Dimorphism in fungal pathogens: *Candida albicans* and *Ustilago maydis* – similar imputs, different outputs. Curr. Op. Microbiol. 4, 214-221.

Steinberg G. and Perez-Martin J. 2007. Ustilago maydis, a new fungal model system for cell biology. Trends in Cell Biology. 18:61-67.

Vitali B., Wasinger V., Brigidi P., Guilhaus M. 2005. A proteomic view of *Bifidobacterium infantis* generated by multi-dimensional chromatography coupled with tandem mass spectrometry. Proteomics. 5.1859–1867.

Vollmeister F., Schipper K., Baumann S., Haag C., Pohlmann T., Stock J. And Feldbrügge M. 2011. Fungal development of the plant pathogen *Ustilago maydis* FEMS microbial Rev 36: 59-77.

Westermeier R., Naven T. and Höpker H. 2008. Proteomic in practice. A guide to successful experiments design 2nd ed. "*foreword*" p. 13.

Zarnack K., Eichhorn H., Kahmann R. And Feldbrügge. 2008. Pheromone regulated target genes respond differentially to MAPK phosphorylation of transcription factor Prf1. Molecular Microbiology. 69: 1041-1053.